Effect of temperature and adhesive defect on repaired structure using composite patch

Mohammed Abdulla, Meftah Hrairi*
Department of Mechanical and Aerospace Engineering, Kulliyyah of Engineering, International Islamic University Malaysia, Kuala Lumpur, Malaysia
hafizabdulla2426@gmail.com, meftah@iium.edu.my

Abdul Aabid
Department of Engineering Management, College of Engineering, Prince Sultan University, Riyadh, Saudi Arabia
aaabid@psu.edu.sa

Nur Azam Abdullah
Department of Mechanical and Aerospace Engineering, Kulliyyah of Engineering, International Islamic University Malaysia, Kuala Lumpur, Malaysia
azam@iium.edu.my

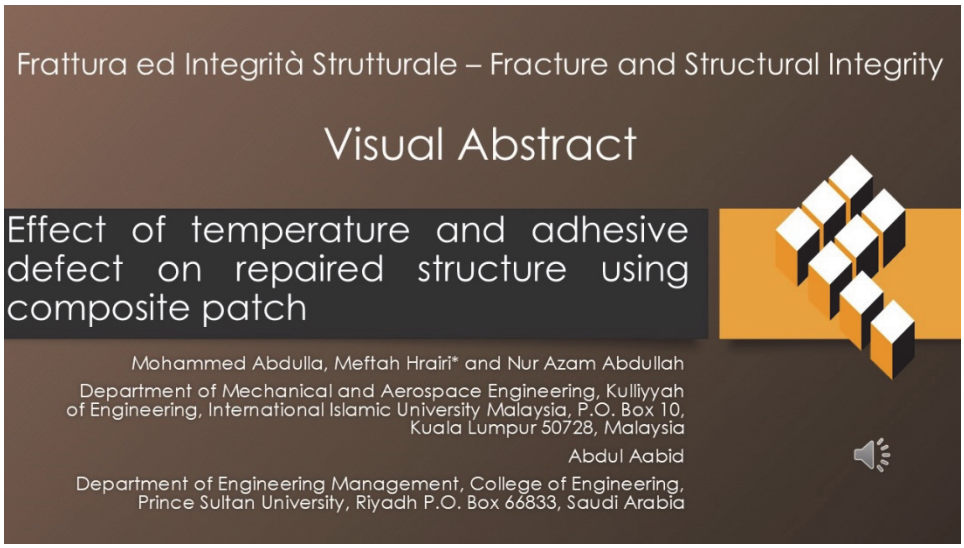

Citation: Abdulla, M., Hrairi, M., Aabid, A., Abdullah, N. A., Effect of temperature and adhesive defect on repaired structure using composite patch, Frattura ed Integrità Strutturale, 71 (2025) 124-150.

Received: 20.08.2024
Accepted: 14.10.2024
Published: 16.10.2024
Issue: 01.2025

KEYWORDS. Aluminium, composite patch, stress intensity factor, finite element stress analysis, thermal analysis, adhesive defect.

INTRODUCTION

Cracks and damage in structural components arise from various factors including mechanical loading, thermal stresses, environmental conditions, and material defects. Mechanical loading, such as cyclic or impact loading, often initiates micro-cracks that can propagate over time due to fatigue, leading to significant structural damage [1]. Fatigue crack initiation results from cyclic slip and plastic deformation, primarily through dislocation activities. These

processes typically occur at stress amplitudes below the yield stress, with surface grains experiencing less constraint compared to subsurface grains, facilitating the formation of slip steps and exposure of fresh material. The initial slip and subsequent strain hardening lead to microcracks that grow with each load cycle, often starting along slip bands and evolving with continued loading.

Thermal stresses, induced by temperature variations, can cause the expansion and contraction of materials, resulting in thermal fatigue and crack initiation [2]. Environmental factors, including corrosion and moisture ingress, can weaken material properties and accelerate crack growth. Additionally, manufacturing defects, such as voids, inclusions, or improper bonding, contribute to the initiation of cracks [3].

Cracks often propagate due to stress concentration at the crack tip, characterized by the stress intensity factor (SIF). When the SIF exceeds a critical value, rapid crack growth occurs, potentially leading to catastrophic failure. Factors influencing crack propagation include the applied stress, material toughness, and the presence of stress concentrators like holes or notches [4]. As cracks grow, stress concentration at the crack tip activates multiple slip systems, altering the crack's growth direction and rate. This growth rate may vary with interactions at grain boundaries and internal material constraints. Initially, crack propagation might show inhomogeneous growth rates due to material barriers, but once the crack has penetrated enough grains, growth becomes more continuous and less influenced by surface conditions, focusing on bulk material properties.

Structural failures can occur despite existing preventive procedures. These failures are often due to human errors such as poor workmanship, use of substandard materials, or errors in stress analysis. While existing procedures are generally sufficient to avoid failure, they may not be followed due to human error, ignorance, or wilful misconduct. Examples include poor workmanship, inappropriate or substandard materials, and operator error, where the appropriate technology and experience are available but not applied [5]. A more challenging type of failure to prevent occurs with the introduction of improved designs, which may have unforeseen factors not anticipated by the designer. New materials, while offering significant advantages, can also present potential problems. Thus, new designs or materials should be extensively tested and analyzed before being placed into service. This approach reduces the frequency of failures but does not eliminate them, as some critical factors may be overlooked during testing and analysis [6].

In the realm of structural engineering and materials science, the repair and rehabilitation of damaged components have emerged as pivotal areas of research and application [7]. The automotive and aerospace industries make substantial use of adhesive bonded joints because of their low specific weights, ability to distribute loads uniformly, and increased design freedom [8].

The fundamental principle behind composite patch repair lies in its ability to reinforce and restore the integrity of a damaged structure by strategically applying composite patches onto the affected areas. These patches effectively redistribute stresses, restrain crack propagation, and improve load-carrying capabilities [9-10]. The versatility of composite materials enables tailor-made solutions that can be adapted to various types of structures, from bridges and buildings to pipelines and aerospace components. A comparative study between elliptical and circular-shaped patches was carried out considering the effect of thermal and mechanical load using the FEM [11]. Findings show that the circular-shaped patch performed well in decreasing the SIF since this shape form results in weaker adhesive tensions than the elliptical shape. To investigate the impact of a corrosive environment on repair effectiveness, cracked aluminium structures were patched with materials including boron/epoxy and graphite/epoxy [12]. This is why salt water was employed. The results showed that boron/epoxy repaired plates produced positive life improvement outcomes while graphite/epoxy repaired plates showed an increase in crack propagation due to corrosive content.

Experimental and numerical research was done to examine the impact of adhesive disbond [13]. It discovered that the number of cycles to failures dropped as adhesive disbond length increased. In another study, FEM was used to investigate how well the repair of edge cracked plate functioned when there was an adhesive defect [14]. Mohammadi et al., [15] studied the impact of patch thickness in repairing a structure with an inclined crack in its centre. It was found that a patch with raising thickness improves repair performance however this statement is true for thicker host structures. The fatigue life was estimated for an edge-cracked plate experimentally for different patch shapes and rectangular-shaped patches outperformed followed by trapezoidal shape. Amari et al., [16], using ABAQUS, performed FEA to identify the best shape of patch among full shape and notched shape for repairing a notched composite plate. The impact of adhesive curing on bonded passive repair using composite patches was studied by [17]. In another study, the impact of the direction of fiber in composite was examined for passive repair [18]. Aabid et al., [19] trained several machine learning algorithms to predict the SIF value in the repair using composite patch.

Based on the literature, it has been proven that the lack of comprehensive investigation into the broader spectrum of thermal conditions and their impact on repair efficiency, alongside the neglect of examining the effect of adhesive disbond under varied loading conditions, has created significant gaps in current research on composite repairs. Therefore, this

study focused on addressing these critical gaps by adopting a pioneering approach to broaden the scope of the investigation. This research was conducted using the Finite Element (FE) method, specifically targeted damage mode I crack type, as it is commonly encountered in real-world structural applications, presenting distinct challenges in crack propagation and repair efficiency. Mode I crack opening displacement is particularly significant in tensile loading, as it directly contributes to failure and consequently affects the load-bearing capacity of the cracked structure [20]. This investigation aimed to explore a wider range of thermal conditions and incorporate both mechanical and thermo-mechanical loading scenarios. Unlike previous investigations, which often overlooked the effects of temperature variations on adhesive defect and repair effectiveness, this study rigorously examined these dynamics. Through advanced computational analysis, it is endeavoured to uncover novel insights into the intricate interactions between temperature changes, composite material behaviour, and structural integrity. The novelty of the current work lies in its comprehensive examination of passive repair techniques for cracked aluminum plates using composite patches under both mechanical and thermo-mechanical loading conditions. This study investigates the influence of adhesive defects and explores various parametric factors affecting repair efficacy in these scenarios. By addressing these critical aspects, this research aims to fill significant gaps in the existing literature and offers valuable insights for optimizing repair strategies, ultimately enhancing the durability and performance of repaired aluminum structures in practical applications.

MATERIAL AND METHODS

Geometric and Finite element model

An aluminum plate with a crack at its centre is repaired using a composite patch bonded through an adhesive is considered for this analysis. A uniaxial tensile load of 1 MPa was applied in the vertical direction (y-direction) of the plate. The dimensions of the plate are as follows: Height = 160 mm, Width = 100 mm, and Thickness = 1 mm. The dimensions for the composite patch and adhesive used to repair the plate are as follows: Height, Hp = Ha = 20 mm, Width Wp = Wa = 40 mm, Thickness Tp = 0.5 mm, and Ta = 0.03 mm, respectively. The selected adhesive thickness of 0.03 mm for the composite patch repair was chosen to ensure compatibility with both the patch and the base plate materials, facilitating effective load transfer while minimizing stress concentrations at the bond interface. This thin adhesive layer is critical for maintaining structural integrity by preventing crack initiation or propagation. A crack of crack length 2a at the center of the plate was modeled throughout the plate thickness and repaired using a single-layer composite patch bonded using adhesive as shown in Fig. 1(a) below. The composite patch in this study has its fibres aligned with the direction of the applied stress, as illustrated in Fig. 1(b). For this study, three different composite patches Boron/epoxy, Graphite/epoxy, and Glass/epoxy have been evaluated each with specific properties detailed in Tab. 1. Furthermore, three different adhesives Araldite 2015, FM73, and AV138 were tested for bonding the composite patch to the plate, with their mechanical and thermal properties detailed in Tab. 2. These adhesives were chosen for their high shear strength and thermal stability. The material properties of the plate and patch are listed in Tab. 1.

Environmental exposure plays a crucial role in the development of adhesive defects. Moisture ingress, for instance, can lead to hydrolysis or plasticization of the adhesive material, weakening the bond and increasing its susceptibility to mechanical damage. Temperature variations can cause differential expansion and contraction between the adhesive and the bonded materials, creating thermal stresses that promote the growth of existing defects or the initiation of new ones.

As these defects grow, they can cause partial or full delamination of the adhesive layer from the substrate, significantly reducing the load transfer capability of the bonded joint [21]. The presence of disbonds or voids within the adhesive layer can significantly affect the stress distribution around the repaired area. Instead of the load being evenly distributed across the adhesive bond, areas with defects concentrate stress, particularly near the crack tip. This concentration of stress can increase the SIF, which is critical in determining the rate of crack propagation. As the SIF increases, the likelihood of crack growth also increases, undermining the effectiveness of the repair.

The specific square voids modeled in this study are representative of common defects that occur in real-world applications, such as those caused by air entrapment during the adhesive application process. These voids typically originate from insufficient adhesive spread, lack of proper pressure during bonding, or the presence of contaminants that prevent complete bonding. Over time, these voids can serve as initiation sites for further delamination, especially under mechanical loading or environmental stress [22].

Furthermore, as the adhesive layer is subjected to cyclic loading, these defects propagate, leading to more extensive delamination and a significant reduction in the overall structural integrity of the repair. This study's focus on square voids in specific locations within the adhesive layer is crucial in understanding how such localized defects can compromise the

effectiveness of composite patch repairs, especially when considering factors such as moisture ingress and temperature variations that can exacerbate these defects.

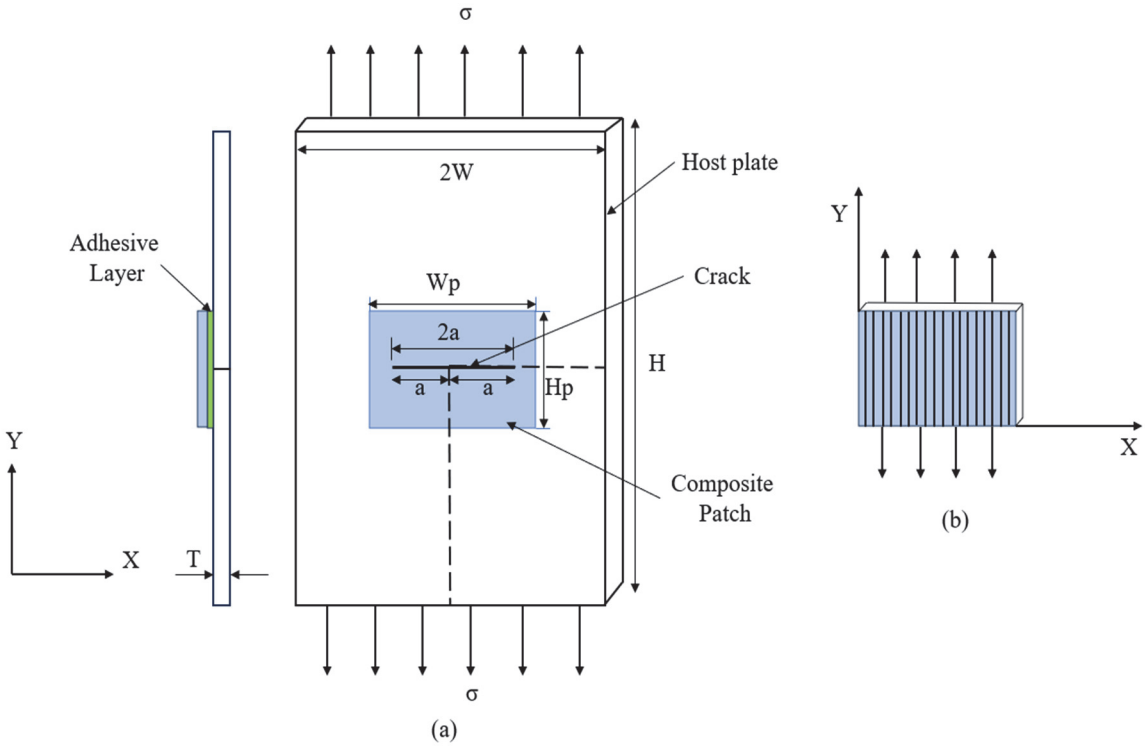

Figure 1: (a) A center cracked plate repaired by composite patch bonded using adhesive (b) Direction of fiber orientation of composite patch.

As shown in Fig. 2 (b) a square void measuring 2 mm × 2 mm has been modeled for every crack length in the adhesive layer at six distinct places. Fig. 2(a) depicts the quarter part of the defect-free adhesive area.

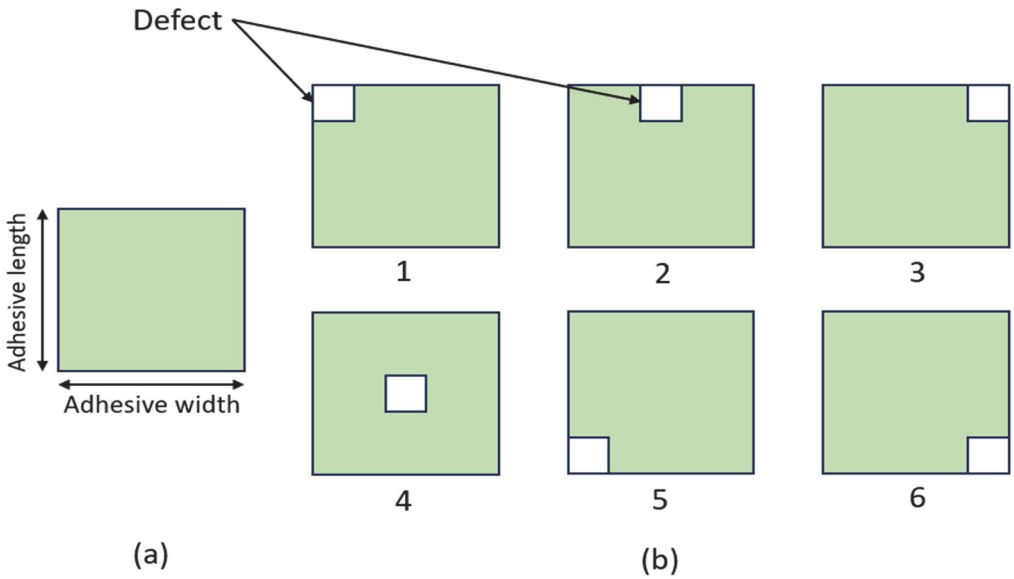

Figure 2: (a) Original quarter adhesive with no defect (b) Adhesive with defect at different locations.

Parameter	Aluminium	Composite patch		
		Boron/epoxy	Graphite/epoxy	Glass/epoxy
Youngs Modulus (E1), GPa	68.95	200	134	50
Youngs Modulus (E2), GPa		19.6	10.3	14.5
Youngs Modulus (E3), GPa		19.6	10.3	14.5
Poison's ratio ν_{12}	0.33	0.3	0.33	0.33
Poison's ratio ν_{13}		0.28	0.33	0.33
Poison's ratio ν_{23}		0.28	0.33	0.33
Shear Modulus (G12), GPa		7.2	5.5	2.56
Shear Modulus (G13), GPa		5.5	5.5	2.56
Shear Modulus (G23), GPa		5.5	3.2	2.24
α_{12} (10^{-6}/°C)	22.5	4.5	-1.2	5.5
α_{13} (10^{-6}/°C)		23	34	15
α_{23} (10^{-6}/°C)		23	34	15

Table 1: Material Properties for host plate and composite patch.

Adhesive	Youngs Modulus (GPa)	Poisson's ratio	Shear Modulus (GPa)	Coefficient of thermal expansion (10^{-6}/°C)
Araldite 2015	5.1	0.345	1.89	85
AV138	4.59	0.47	1.56	67
FM73	1.83	0.32	0.96	50

Table 2: Material Properties for adhesives.

Finite Element Modeling

For analysis, the commercial finite element code ANSYS was employed, where three bodies were modeled: the cracked plate, adhesive, and patch, using SOLID 186 elements. SOLID 186 is a 20-node higher-order element used for modeling 3-dimensional bodies. Due to symmetry, only the bottom half of the plate was modeled. A total of 19,992 elements were used for modeling the cracked plate, 3,854 elements for the adhesive, and 11,562 elements for the patch. Using the "KSCONC" command, the key point of the crack tip was concentrated, and the mesh was refined to accurately capture the SIF at the fracture point. The number of elements around the circumference of the fracture point was set to 10. After applying the boundary conditions, the solution was obtained using the SOLVE command. The displacement extrapolation method was used to accurately measure the SIF, utilizing the displacements of nodes near the fracture tip, where the stress and strain fields change more rapidly. Fig. 3(a) depicts the crack face and crack front, while singular elements used to describe the displacement at the fracture tip are shown in Fig. 3(b). Fig. 4 depicts the meshed body of the repaired plate.

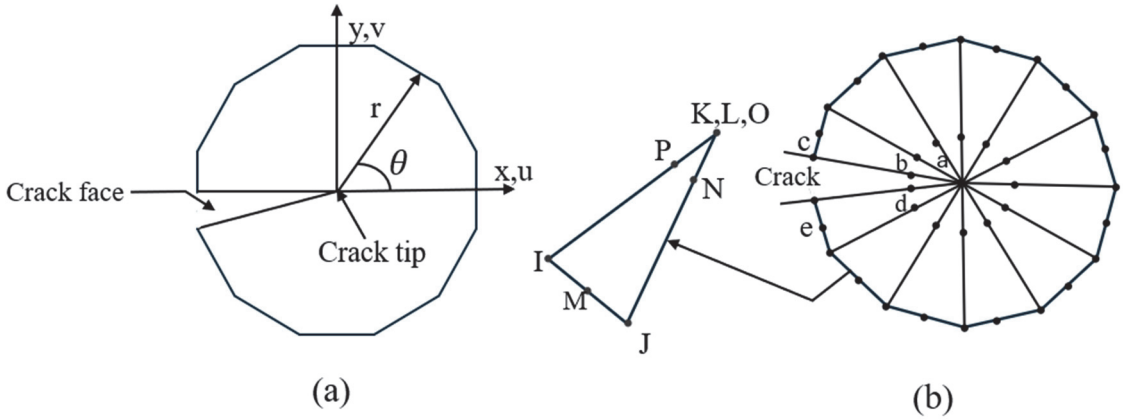

Figure 3: (a) Crack face and crack tip (b) singular elements close to the fracture point.

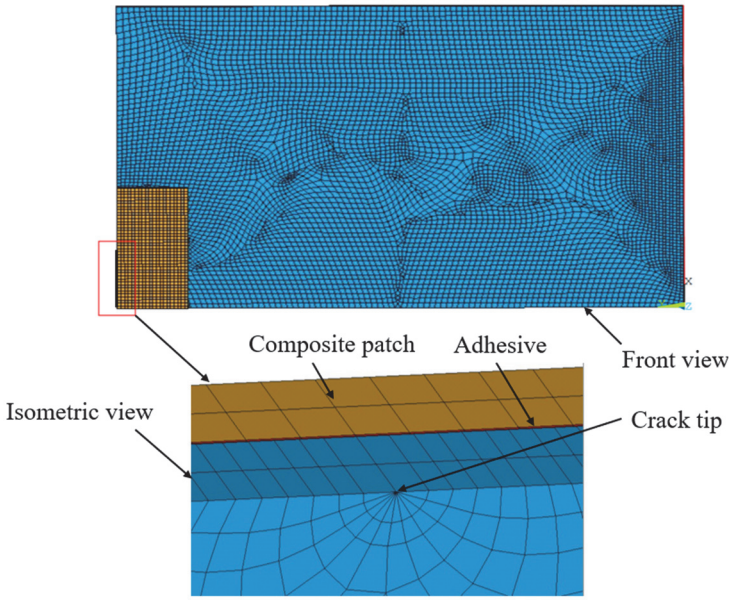

Figure 4: Meshed view of plate.

Stress and Displacement Fields Near the Crack Tip

The stress field near the crack tip in a linear elastic material is characterized by the Mode I (opening mode) stress intensity factor K_I. The stress components in polar coordinates (r,θ) around the crack tip are given in Eqn. (1) [4]:

$$\sigma_{ij}(r,\theta)=\frac{K_I}{\sqrt{2\pi r}}f_{ij}(\theta) \tag{1}$$

where σ_{ij} is the stress components, r is the distance from the crack tip, and θ is the angle with respect to the crack plane. The functions $f_{ij}(\theta)$ for mode I are provided in Eqns. (2), (3) and (4) as follows:

$$\sigma_{xx}(r,\theta)=\frac{K_I}{\sqrt{2\pi r}}\cos\frac{\theta}{2}\left[1-\sin\frac{\theta}{2}\sin\frac{3\theta}{2}\right] \tag{2}$$

$$\sigma_{yy}(r,\theta)=\frac{K_I}{\sqrt{2\pi r}}\cos\frac{\theta}{2}\left[1+\sin\frac{\theta}{2}\sin\frac{3\theta}{2}\right] \tag{3}$$

$$\tau_{xy}(r,\theta)=\frac{K_I}{\sqrt{2\pi r}}\cos\frac{\theta}{2}\sin\frac{\theta}{2}\cos\frac{3\theta}{2} \tag{4}$$

The displacement components near the crack tip can be expressed as in Eqn. (5) and (6) [23]:

$$u_x(r,\theta)=\frac{K_I}{E'}\sqrt{\frac{r}{2\pi}}\left(k-1+2\sin^2\left(\frac{\theta}{2}\right)\right)\cos\left(\frac{\theta}{2}\right) \tag{5}$$

$$u_y(r,\theta)=\frac{K_I}{E'}\sqrt{\frac{r}{2\pi}}\left(k-1+2\cos^2\left(\frac{\theta}{2}\right)\right)\sin\left(\frac{\theta}{2}\right) \tag{6}$$

where u_x and u_y are the displacement components in the x and y directions respectively. E' is the effective Young's modulus, given by E' = E for plane stress conditions, and k is a parameter that depends on the material properties and is given by k = 3-ν for plane stress, where ν is Poison's ratio.

Mesh sensitivity analysis

Mesh sensitivity analysis in ANSYS, or any FEA software, is a technique used to evaluate how the quality and density of the finite element mesh (the division of the geometry into small elements) affects the accuracy of the simulation results. It helps in determining the optimal mesh size and quality to ensure that the FEA results are reliable and representative of the actual behaviour of the system being analyzed. In a comprehensive mesh sensitivity analysis, three distinct mesh configurations were rigorously assessed: coarse, intermediate, and fine. The objective was to discern the impact of varying the number of elements on the SIF while concurrently recording the computational time for each case. Remarkably, the results demonstrated that the intermediate mesh configuration yielded SIF values that closely paralleled those of the fine mesh, all while accomplishing the level of resolution deemed adequate for the analysis. Intriguingly, this achievement in result fidelity did not come at the cost of computational efficiency. The intermediate mesh configuration demanded a substantially reduced computational time, approximately 50% less than the fine mesh configuration, making it an attractive and pragmatic choice for this specific analysis as depicted in Fig. 5. This finding underscores the optimization potential inherent in judiciously selecting an intermediate mesh, as it balances computational resource utilization and accurate SIF determination, thereby expediting the analysis without compromising the quality of results.

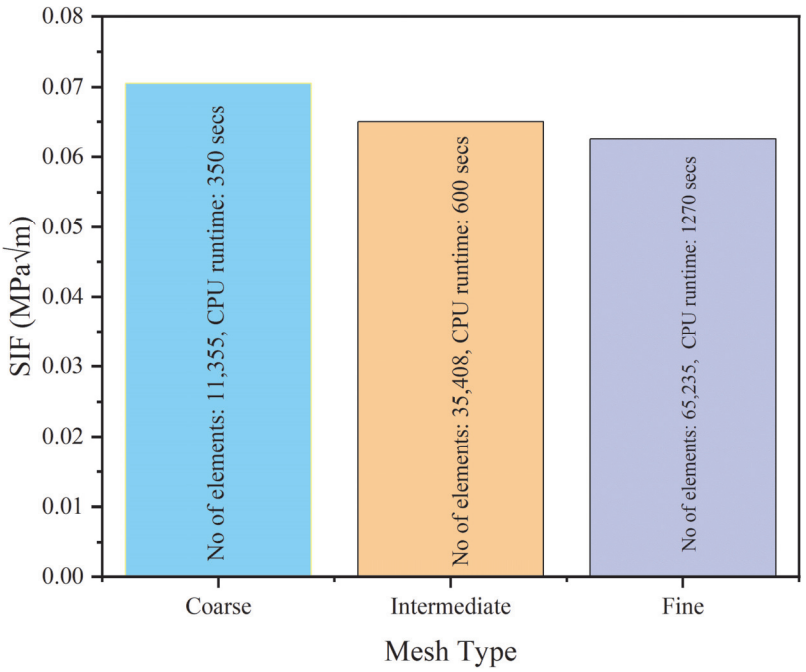

Figure 5: Mesh sensitivity test.

VALIDATION OF THE MODEL

Validation of unrepaired plate

For the unrepaired plate, a centre cracked plate with a crack length of 10 mm was subjected to an external tensile load of 50 MPa on its top and bottom ends and the SIF was calculated. The analytical Eqn.. (7) from [24] was used to validate the FE results as mentioned below.

$$K_I = \sigma\sqrt{\pi a}\, F(a/b) \tag{7}$$

From Tab. 3, it can be observed that for the unrepaired case, the difference in SIF between the present FE results and the theoretical results is 2.78%.

Case	Simulation results	Theoretical results	Percentage error
Unrepaired	9.109	8.862	2.78 %

Table 3: Validation of current results with theoretical ones for unrepaired plate.

Additionally, the current study for the unrepaired plate was validated against the numerical investigation conducted by [25] on a center-cracked rectangular aluminum 2024-T3 plate under tensile loading. The comparison with the present FE results showed good agreement as depicted in Fig. 6.

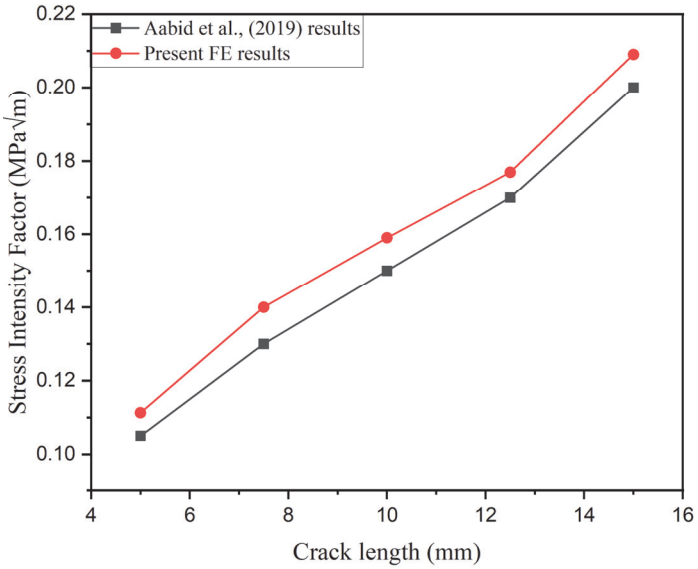

Figure 6: Validation of current results of unrepaired plate with simulation from the literature.

Mathematical Formulation for Stress Intensity Factor in Repaired Plate

In this study, the SIF for the repaired centre-cracked plate was determined using a detailed formulation that accounts for the geometric and mechanical parameters of the adhesive and the composite patch. This approach is based on the Rose model, which is widely used for such analyses and provides a more accurate representation of the SIF for repaired plates compared to classic formulations for unrepaired plates.

Rose Model for Stress Intensity Factor in Centre-Cracked Plate

The Rose model provides a means to account for the effect of the composite patch and adhesive layer on the SIF. The SIF for a repaired centre-cracked plate can be expressed as in Equation (8) [26]:

$$K_R = \sigma_0 \sqrt{\pi\Lambda \frac{a}{a+\Lambda}} \tag{8}$$

where σ_0 is the reduced stress in the plate at the location of the crack proportional to the applied stress, a is the crack length, and Λ is the characteristic crack length.
The parameter Λ is given by Eqn. (9):

$$\pi\Lambda = \left(1+\frac{1}{S}\right)\beta E_P t_P \frac{t_a}{G_A} \tag{9}$$

where S is the stiffness ratio between the repaired and unrepaired sections of the plate and β is a parameter that depends on the properties and dimensions of the adhesive and the patch and is given by Eqn. (10) [27]:

$$\beta^2 = \frac{G_A}{t_a}\left(\frac{1}{E_P t_P}+\frac{1}{E_R t_R}\right) \tag{10}$$

E_p is the Young's modulus of the plate, t_p is the thickness of the plate, E_R is the Youngs modulus of reinforcement/patch, t_R is the thickness of the patch, t_a is the thickness of the adhesive and G_A is the shear modulus of the adhesive.

The upper bound for the stress intensity factor is given by the Eqn. (11):

$$K_{\infty} = \sigma_0 \sqrt{\pi \Lambda} \tag{11}$$

Validation of repaired plate

To validate the accuracy of finite element results obtained using ANSYS for the repaired plate, the work performed by [16] was replicated, which involved the repair of a centre-cracked plate with a crack of length ranging from 5-40 mm using a Boron/epoxy patch bonded with FM73 adhesive. The results showed a good agreement between the FE model and the experimental SIF as can be seen in Fig. 7. These results indicate that the ANSYS code is capable of accurately predicting the SIF for both unrepaired and repaired cases. The relatively small difference in SIF between my results and the literature is likely due to differences in the meshing.

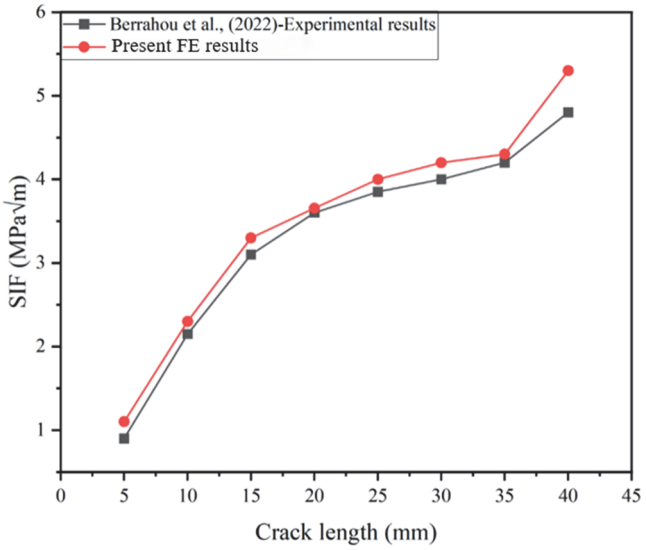

Figure 7: Simulation SIF vs Experimental SIF for repaired plate.

RESULTS AND DISCUSSIONS

In this section, results obtained from FE analysis are explained. The SIF at the crack tip was determined using the "KCALC" command. After applying both mechanical and thermal loads, the model is solved using the SOLVE command. For the calculation of SIF, the displacement extrapolation method is employed. The initial phase involves setting up a workplace and creating a local coordinate system (CS) using three nodes, with the first node at the crack tip and two additional nodes forming a triangular shape. A path along the crack face is defined, with the crack face aligned parallel to the x-axis and the y-axis perpendicular to the crack face. The path starts at the crack-tip node, followed by a node near the crack tip, and a final node farther from the crack tip. This setup allows for accurate SIF calculation through the displacement extrapolation method, providing essential insights into the fracture mechanics of the repaired structure under different loading conditions. The current study under mechanical loading assumes the absence of thermal residual stresses in the model and maintains the model temperature at 20℃ without considering any thermal strains.

Mechanical loading

A noteworthy pattern in the SIF for cracked plates was noted during the investigation. Specifically, the SIF for unrepaired plates showed a consistent linear increase with crack length, indicating higher stress concentrations at the crack tip as the fracture progressed. On the other hand, the SIF was significantly decreased upon the addition of a Boron/epoxy patch, which was adhered to with FM73 adhesive. This resulted in a noteworthy 62% decrease, as illustrated in Fig. 8. With an increase in crack length, this SIF decrease became noticeably more pronounced, exhibiting an asymptotic behaviour where the patch's ability to lower the SIF gets better as the fracture gets longer.

The observed reduction in SIF can be attributed to the composite patch's improved structural integrity, which plays a crucial role in stress redistribution. By adding a material with a different stiffness and modulus than the underlying material, the patch modifies the local mechanical properties of the cracked plate. The tension around the crack tip is spread across a wider area due to this change in material properties. More specifically, by effectively dispersing the applied load across a larger area, the stiffness of the patch lowers the stress concentration at the fracture tip. This reduces the localized tension at the crack tip, preventing the crack from spreading farther.
Additionally, by adding more reinforcement, the composite patch raises the restored plate's overall structural resilience. This reinforcement improves the plate's structural load-bearing capability while also slowing the growth of cracks. Longer cracks provide a greater degree of SIF reduction efficacy for the composite patch, indicating that it is appropriate for more severe damage scenarios and highlighting the significance of using strong repair methods in essential structural applications. This thorough comprehension of the composite patch's ability to reduce cracks and redistribute stress emphasizes the patch's important contribution to enhancing the resilience and safety of repaired structures.

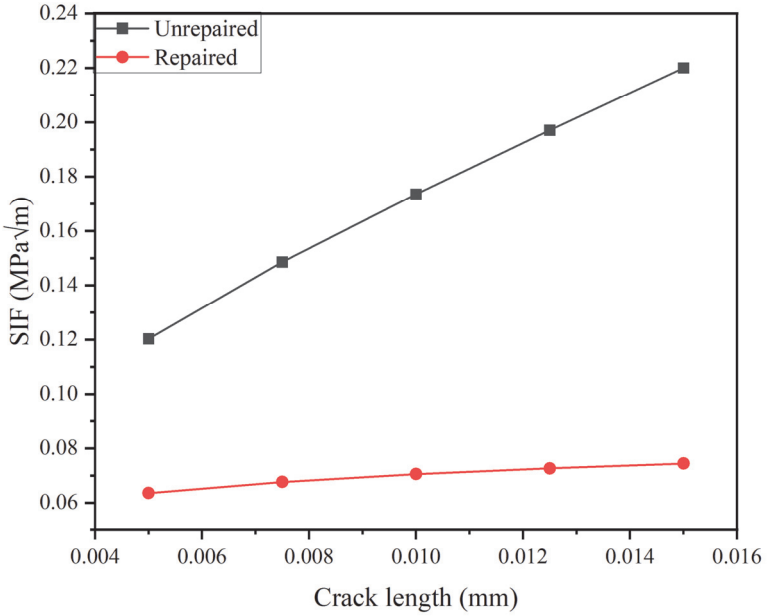

Figure 8: SIF vs Crack length.

Patch thickness

A consistent inverse relationship between the composite patch thickness and SIF was noted during the mechanical loading analysis. In particular, Fig. 9 shows that increasing the thickness of the boron/epoxy composite patch, bonded with FM73 adhesive, from 0.5 mm to 1.25 mm resulted in a significant 21% decrease in SIF over a range of crack lengths. There are several important reasons for this SIF decline that occurs as patch thickness increases. Through the effective reduction of stress concentration at the fracture tip, a thicker patch improves the structural integrity of the repaired area by dispersing the applied load over a greater cross-sectional area. The improved crack bridging mechanism where the fibres in the composite material interface with the crack surfaces, preventing the crack opening and so reducing SIF is made possible by the extra material in a thicker patch, which increases the stiffness of the patched region. The driving force behind crack propagation is lessened as a result of this redistribution of stress, which also lowers the localized strain energy at the crack tip. Furthermore, the patch's greater thickness reduces the possibility of delamination between the composite layers, a crucial element that, if left unchecked, might worsen the development of cracks. The thicker patch's increased stiffness makes the structure more resilient to deformation under load, which lowers the stress-strain factor even more. Additionally, this enhanced load transfer mechanism postpones the commencement of rapid fracture growth, especially in situations where fatigue-induced crack propagation is the main cause for concern in cyclic loading circumstances. Therefore, thicker patches are important for optimizing structural engineering repair operations since they slow down the propagation of cracks and increase the fatigue life and overall durability of the restored structure by lowering the SIF. While increasing patch thickness leads to a significant initial reduction in SIF, the reduction becomes less pronounced as thickness continues to increase. This behavior follows an exponential decay pattern, meaning the SIF reduction slows down, providing diminishing returns with further increases in patch thickness.

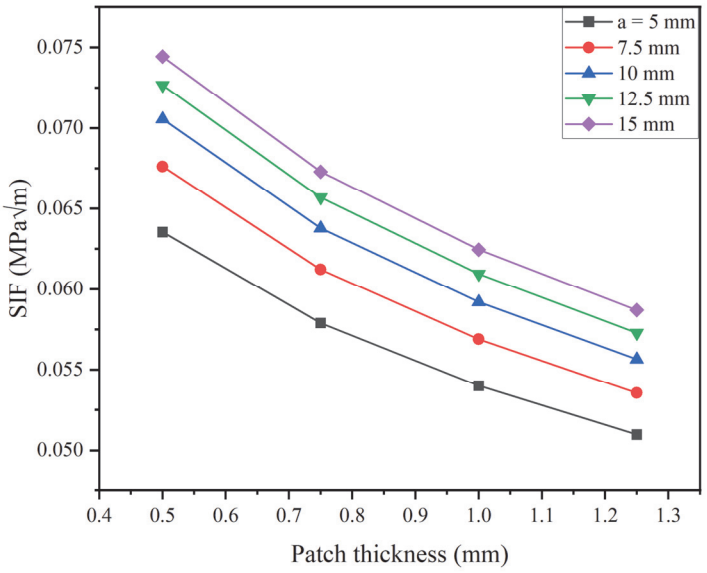

Figure 9: SIF for different patch thicknesses under mechanical loading.

Patch Size

A distinct pattern emerged when examining the SIF for a 10 mm crack repaired with a composite patch under mechanical loading concerning different patch sizes: the SIF decreased as the patch size increased, as illustrated in Fig. 10. The improved load-bearing capability and stress distribution provided by the larger patches are responsible for this SIF decrease. In particular, larger patches reduce the localized stress concentration at the fracture tip because they have a wider surface area across which the mechanical stresses can be spread. This behaviour is based on the basic ideas of fracture mechanics which state that the stress environment surrounding a crack change when a composite patch is applied. Because larger patches can involve more of the surrounding material in load transmission, they are more effective in changing the stress distribution by lessening the intensity of the stress singularity at the crack tip. When the composite material is placed over a larger area, its strength and stiffness aid to absorb a higher percentage of the applied load, which lessens the strain on the cracked region and, as a result, lowers the SIF. Because of their high modulus of elasticity, which improves stiffness and resistance to deformation under load, composite materials exhibit this effect more strongly. A clear inverse correlation exists between patch size and SIF, where the SIF diminishes as patch size increases.

Furthermore, a more even stress distribution throughout the adhesive layer and the contact between the patch and the base material is facilitated by the larger patch size. Because of this uniformity in stress distribution, there is a lower chance of adhesive failure, which is sometimes a crucial component in how well patch repairs work. Overall, the larger patches improve the structural integrity of the repaired plate by reducing stress concentrations and so reducing the likelihood of additional fracture propagation.

Furthermore, a significant factor in evaluating the success of the repair is the relationship between the crack length and the patch size. When the patch size grows for a crack that is 10 mm in size, it can bridge the crack more successfully and lower the SIF by dispersing the load farther from the crack tip and across a larger region. A mathematical description of this phenomenon may be found in the reduction of the SIF, which is inversely proportional to the effective area of the load distribution that the patch provides.

Patch materials

During an investigation of different patch materials under mechanical loading, it was found that boron/epoxy exhibited the lowest SIF values, followed by graphite/epoxy, with glass/epoxy demonstrating the highest SIF values as illustrated in Fig. 11. This trend can be attributed to the distinct material properties and reinforcement mechanisms inherent to each material. Boron/epoxy composites, renowned for their exceptional stiffness and high tensile strength, feature Young's modulus of 200 GPa. The incorporation of boron fibres significantly enhances load-carrying capabilities, reducing stress concentrations within the material during mechanical loading. As a result, the SIF values for boron/epoxy composites were notably lower, indicating improved resistance to crack propagation.

In contrast, graphite/epoxy composites, with Young's modulus of 134 GPa, possess advantageous mechanical properties but do not match the tensile strength and load-carrying capacity of boron fibres. Consequently, their SIF values were

intermediate, suggesting moderate resistance to crack propagation. The graphite fibres provide a good balance of stiffness and strength, which contributes to better performance compared to glass/epoxy but not as effectively as boron/epoxy.
Glass/epoxy composites, with Young's modulus of 50 GPa, exhibited the highest SIF values due to their lower mechanical properties. The reduced tensile strength and stiffness of glass/epoxy result in higher stress concentrations at crack tips under mechanical loading, leading to elevated SIF values and lower resistance to crack propagation. The inherent material limitations of glass/epoxy composites mean that they are less effective in distributing the applied stresses, thus increasing the likelihood of crack growth under mechanical loading.
Overall, the findings highlight the superior performance of boron/epoxy in reducing SIF under mechanical loading and enhancing the structural integrity of repaired plates, making it the most effective material among those studied.

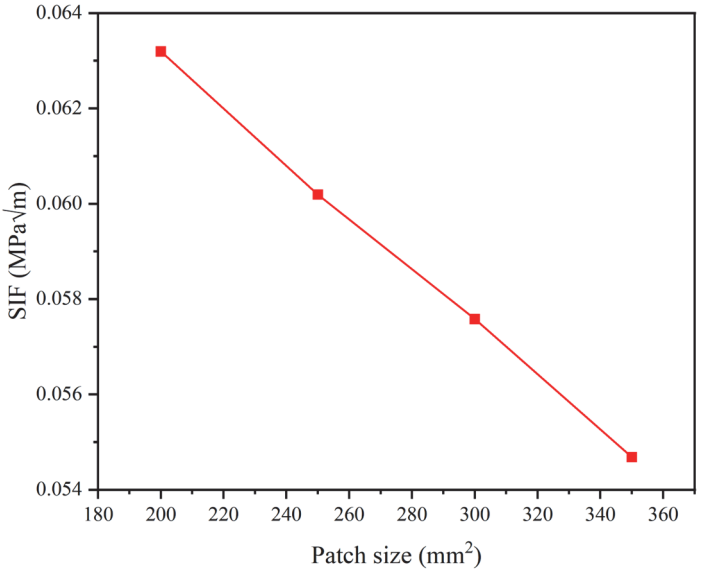

Figure 10: SIF for different patch sizes under mechanical loading.

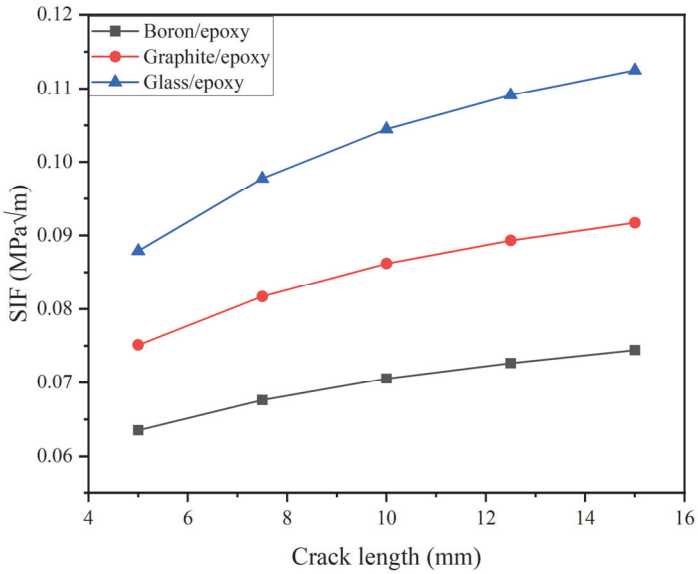

Figure 11: SIF for different patch materials under mechanical loading.

Adhesive materials

A boron/epoxy composite patch was applied to a plate with a crack length of 10 mm to evaluate three different adhesive materials: Araldite 2015, AV138, and FM73. The tests were conducted under mechanical loading conditions. The result, as shown in Fig. 12, demonstrated that FM73 exhibited the highest SIF value among the adhesives tested, whereas Araldite

2015 showed the lowest SIF value, closely followed by AV138.

Although this investigation focused on boron/epoxy patches, it is important to note that the behavior of different adhesives is generally consistent across various composite materials. The performance of adhesive materials is largely independent of the patch type, as their mechanical properties influence stress distribution and crack propagation similarly. Araldite 2015 outperformed others due to its superior stiffness and mechanical properties, enabling it to more effectively transfer and distribute stress across the bonded interface. Due to this effective stress transfer, stress concentrations at the crack tip are minimized, reducing the SIF and thereby increasing the structure's resistance to crack propagation.

Araldite 2015 and AV138 have similar stress distribution capacities, as evidenced by the comparatively minor variation in SIF values between them; nevertheless, AV138 is marginally less effective. This indicates that Araldite 2015 is slightly superior to AV138 in terms of managing and dissipating stress under mechanical loading, even if AV138 is still a feasible alternative for lowering SIF. Alternatively, FM73 seems to have less stiffness, which leads to more stress concentration at the fracture tip. It also showed much higher SIF values. As a result, SIF levels are raised and the ability to stop fracture formation is diminished.

The significance of adhesive material properties especially stiffness in affecting the SIF values in composite-repaired structures is highlighted by this comparative investigation. Araldite 2015's capacity to reduce SIF demonstrates how well it enhances the structural integrity of the repaired plate, which makes it a better option for applications where mechanical loading is an issue. The impact of adhesive stiffness on overall stress distribution and crack propagation resistance is further demonstrated by the notable difference in SIF between Araldite 2015 and FM73. This highlights the significance of choosing an appropriate adhesive material to guarantee the longevity and safety of repaired structures. Notably, a study conducted by Aabid et al., [25] corroborated the current findings, revealing similar trends in adhesive performance, thereby reinforcing the validity of the current work.

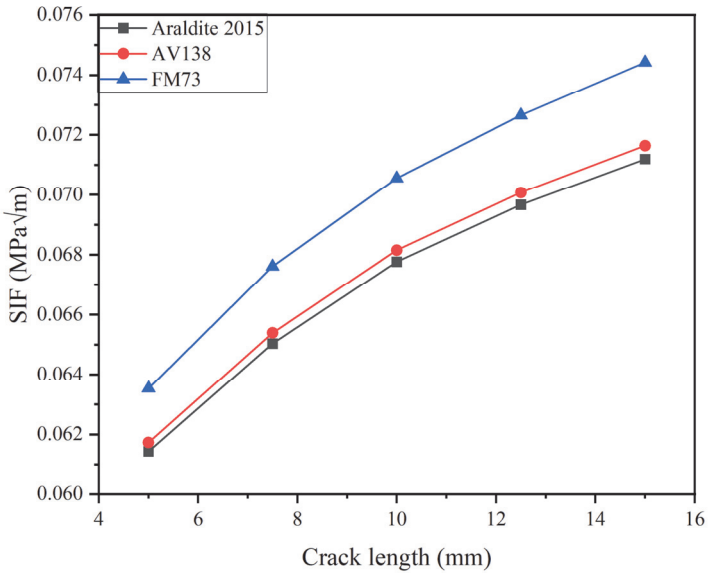

Figure 12: SIF for different adhesives under mechanical loading.

Effect of the existence of a defect in adhesive

This section presents the results of a study on the effect of adhesive defects on the SIF in structures repaired with composite materials. When defects exist in the adhesive layer, as is shown in Fig. 13, the SIF can increase significantly, especially if the defect is in the crack region or close to the patch's free edges. The discontinuities caused by the defect make these locations more vulnerable to higher stress concentrations. Interestingly, the SIF is maximized when a defect is present along the length of the crack, particularly at position 2, which is in line with the crack tip. In this case, the defect increases the stress concentration at the crack tip and raises the possibility that the crack will propagate by impeding the effective transmission of stress from the plate to the patch.

Conversely, the adhesive layer's position 4, which is where the defect is centrally positioned, results in the lowest SIF values. Because the load is distributed more equally throughout the intact adhesive portions in this position, the defect lessens the disruption to stress distribution. Because of the more even distribution of stress, there is less stress concentration at crucial sites, which lowers the SIF. The SIF, for example, is highest at position 2 near the crack tip at a

fracture length of 10 mm, but it reduces when the defect is at position 4 within the adhesive layer, away from places where the maximum stress concentration is present.
These results emphasize how crucial adhesive quality is to patch repairs' overall efficacy. Stress distribution can be significantly altered by the location and degree of adhesive defect, which can compromise the structural integrity of the repair. To ensure the long-term reliability of composite repairs and eventually create safer and more resilient structures, it is imperative to comprehend the influence of adhesive defects.

Comparison of adhesive defect cases with defect free case

In the analysis of the influence of adhesive defects on the SIF, significant variations depending on the defect location relative to the crack was observed, as illustrated in Fig. 13. The SIF values for repaired plates with no adhesive defects consistently exhibited the lowest values across all crack lengths, underscoring the composite patch's effectiveness in mitigating stress concentration and enhancing structural integrity. The presence of adhesive defects resulted in elevated SIF values, with the extent of the increase dependent on the defect location. The most pronounced increase in SIF was observed when the defect was located at position 2, precisely at the crack tip. For a crack length of 10 mm, the SIF reached its peak value due to the defect's impediment of stress transfer from the plate to the patch, leading to heightened concentration at the crack tip. The irregularity of the blue triangle curve in Fig. 13 for defect location 2 reflects this sharp increase in stress concentration. As stress accumulates at the crack tip, it reaches a peak and then redistributes once the defect is surpassed, resulting in the observed fluctuations. This redistribution is less pronounced at other defect locations, where stress transfer is more uniform. Furthermore, for a crack length of 15 mm, the SIF was notably high when the defect was at location 3, which can be explained by the fact that at this crack length, the patch already bears a substantial portion of the stress. The presence of a defect at the patch corner means only a small portion of the patch remains effective in transferring stress, significantly reducing the patch's load-bearing capacity and leading to increased stress concentration at the crack tip. Conversely, the lowest SIF values among the defect cases were observed when the defect was positioned at location 4, the centre of the adhesive layer. For a 15 mm crack length, the SIF was the lowest when the defect was centrally located, minimizing stress concentration due to more uniform stress distribution across the adhesive layer and the composite patch.

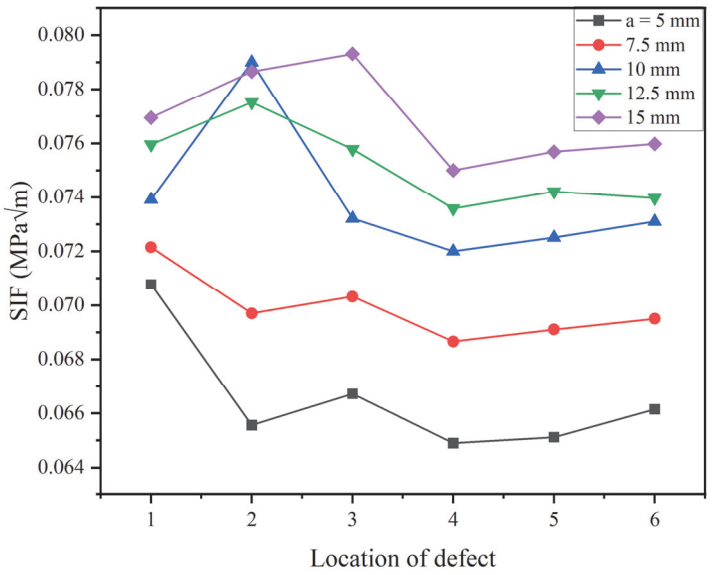

Figure 13: Effect of adhesive defect on SIF under mechanical loading.

Fig. 14 illustrates the significant changes found based on the location of the adhesive defect about the fracture in the extensive research of the effect of the adhesive defect on the SIF. All crack lengths showed that the lowest SIF values were consistently found on repaired plates that did not have any adhesive defect. This result highlights how well the composite patch disperses stress and lowers stress concentrations at the crack tip, improving the structural integrity of the plates that have been repaired. Adhesive defects, on the other hand, dramatically changed the stress distribution and raised SIF values. The location of the defect within the adhesive layer had a significant impact on how much of an increase it was. The position of the defect at position 2, right at the crack tip, showed the greatest increase in SIF. The most

substantial rise in SIF was observed at defect position 2, located directly at the crack tip, particularly for a crack length of 10 mm. This defect acted as a stress concentrator, disrupting smooth stress transfer between the plate and patch, leading to localized stress accumulation and a significant SIF peak. The irregularities in the blue triangle curve in Fig. 14 reflect this strong interaction between the defect and the crack tip. After partial redistribution of stress around the defect, a slight reduction in SIF occurs, resulting in the observed non-linear behavior. This irregularity is specific to this crack length and defect location due to the critical stress concentration formed here. At a crack length of 15 mm, the defect at position 3, near the patch's corner, led to a similarly high SIF value. With the increased strain on the patch at this fracture length, the defect compounded the stress demand, further reducing the patch's load-bearing capability and concentrating stress at the crack tip.

In contrast, the lowest SIF values among defective cases occurred when the defect was located at position 4, the center of the adhesive layer. This position allowed a more uniform stress distribution through the adhesive layer and composite patch, minimizing stress concentrations for a crack length of 15 mm. As the defect is centrally located, it does not significantly interfere with stress flow between the plate and the patch, maintaining overall structural integrity and explaining the lower SIF values.

The comparative study revealed that the SIF values at the crucial fault areas (positions 2 and 3) were almost 20% more than those found in plates that had been fixed without any defect. This significant variation emphasizes how adhesive flaws have a crucial impact on the structural integrity of composite-repaired plates. Defects can seriously hinder the patch's capacity to successfully lower the SIF, particularly in areas that are vital for stress transfer. This analysis emphasizes how crucial it is to apply adhesive precisely and maintain quality control during repair procedures to prevent errors, especially in regions where they could seriously affect stress distribution and reduce the effectiveness of the repair.

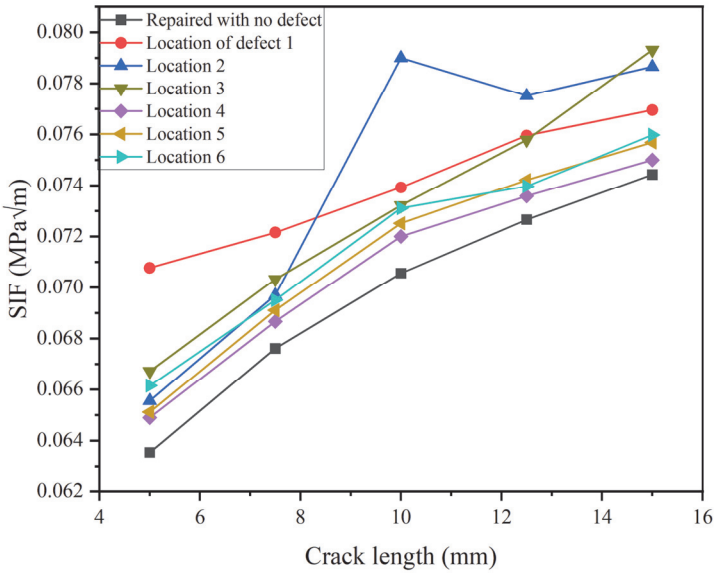

Figure 14: SIF for different defect cases in adhesive and defect-free repair.

Thermo-mechanical loading: under positive temperature

For positive temperature variations, the model was analyzed by uniformly distributing temperatures from 20℃ to 110℃ across all nodes, with a reference temperature of 20℃ for thermal strain calculations. This method enabled us to evaluate the structural response under varying thermal conditions and understand the effect of positive temperature differentials on the SIF at the crack tip.

This comprehensive investigation into positive temperature effects revealed that the SIF consistently increased with rising temperatures. At the baseline of 20℃, there is no thermal strain, and the SIF remains constant for any crack length, as illustrated in Fig. 15. This occurs because only mechanical loading influences the plate at this temperature, which is efficiently distributed to the patch.

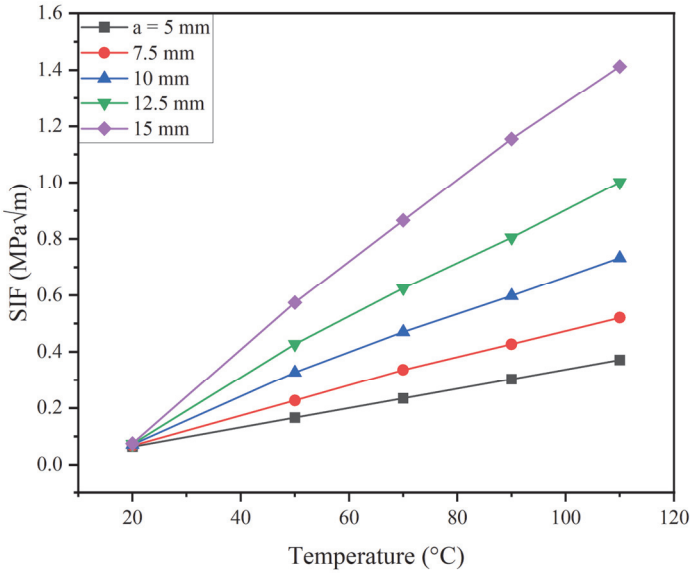

Figure 15: SIF under positive temperature.

When temperatures exceed 20℃, thermal expansion occurs, and aluminium, with its higher coefficient of thermal expansion compared to the composite patch, undergoes more significant expansion. This differential expansion generates tensile stresses in the aluminium, encouraging crack growth. As the temperature rises, the aluminium expands more than the composite patch, creating tensile stresses within the aluminium and compressive stresses within the patch. The tensile stress in the aluminium further opens the crack and amplifies the stress concentration, potentially promoting more rapid crack growth. Although the patches cannot fully govern the overall expansion of aluminium, they effectively limit its free movement through the adhesive bond. Thus, the tensile stress in aluminium outweighs the compressive stresses in the patches, resulting in an increased SIF.

This detailed interplay between thermal and mechanical stresses underscores the critical impact of positive temperature variations on the structural integrity of the repaired plate. The augmentation in stress concentration due to thermal stresses, combined with mechanical loading, results in a more pronounced increase in SIF with increasing crack length. This comprehensive understanding is essential for evaluating the performance of repaired structures under thermal loading conditions.

Thermo-mechanical loading: under negative temperature

For negative temperature variations, the model was analyzed by uniformly distributing temperatures from -90℃ to 0℃ across all nodes, maintaining 20℃ as the reference temperature for thermal strain calculations. This approach allowed us to evaluate the structural response under decreasing thermal conditions and assess the impact of negative temperature differentials on the SIF at the crack tip.

This investigation into the effects of negative temperatures showed a consistent increase in the SIF with decreasing temperatures. As temperatures drop below 20℃, the differing thermal expansion coefficients between the composite patch and the aluminium plate become crucial. Aluminium contracts more than the composite when cooled due to its higher coefficient of thermal expansion. This differential contraction generates localized tensile stresses at the crack tip, intensifying stress concentration. During cooling, aluminium, with its higher coefficient of thermal expansion, undergoes more significant contraction compared to the composite patch. The composite patch, having a lower coefficient of thermal expansion, contracts less during cooling, creating a scenario where the composite material acts as a restraining force on the contracting aluminium plate. This dynamic results in the composite effectively limiting the free contraction of the aluminium plate through the adhesive bond, introducing a complex interplay of forces within the structure.

The consequence of this interaction is the generation of tensile loads experienced by the aluminium plate. While aluminium naturally contracts during cooling, the presence of the composite imposes restrictions, leading to internal stresses within the structure. These thermal tensile stresses increase crack propagation and contribute to a notable increase in the SIF at the crack tip. The more significant the temperature drop, the greater the differential contraction and the more pronounced the thermal stresses, thereby increasing the SIF. The negative temperature conditions intensify the contraction of aluminium, and the restraining effect of the composite amplifies internal stresses, resulting in elevated SIF

values. Understanding this intricate relationship is crucial for assessing the structural response under varying thermal conditions, providing valuable insights for materials and design considerations in real-world applications. This detailed analysis highlights the critical influence of negative temperature variations on the structural integrity of the repaired plate, showing how thermal contraction exacerbates stress concentrations at the crack tip and leads to higher SIF values as can be seen in Fig. 16.

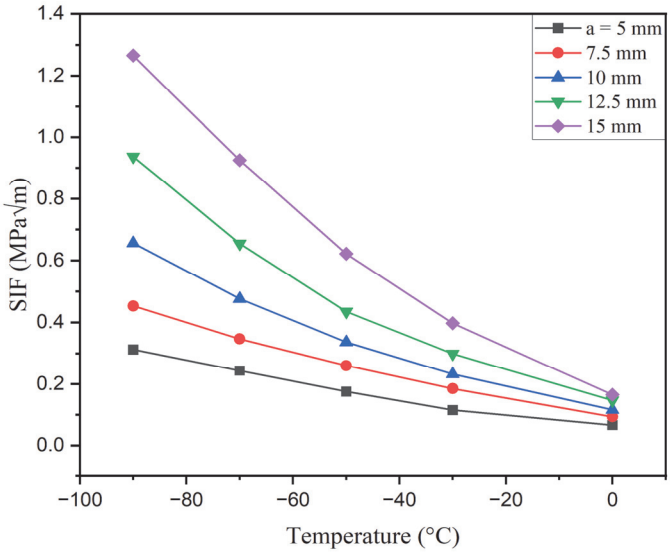

Figure 16: SIF under negative temperature.

Patch thickness

In a comprehensive analysis encompassing both thermo-mechanical and mechanical loading scenarios, a striking disparity in the behaviour of SIF concerning patch thickness was observed. Under thermo-mechanical loading conditions, it became evident that an increase in patch thickness directly correlated with an escalation in SIF at the crack tip. At a relatively modest temperature of 30℃, the SIF values exhibited minimal disparity among various patch thicknesses, denoting only marginal increments. However, as the temperature was elevated to 110℃, a more pronounced discrepancy in SIF values emerged when comparing different patch thicknesses to the configuration with the least thickness of 0.5 mm increased to 0.75 mm, then to 1 mm and the highest thickness of 1.25 mm, resulting in SIF increments of 18%, 36%, and 53% as shown in Fig. 17 respectively.

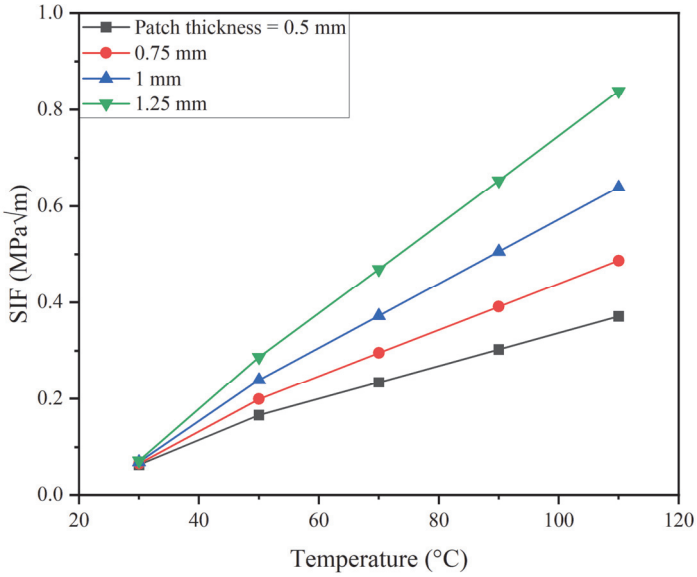

Figure 17: SIF for different patch thicknesses under thermo-mechanical loading.

The underlying reason for this observed trend is rooted in the complex interplay of thermal expansion and thermal gradients. With increased patch thickness, a larger cross-sectional area is subjected to thermal loads, leading to greater thermal expansion and, consequently, elevated thermal stress. This heightened thermal stress, coupled with differential expansion between the patch material and the host structure, results in augmented SIF values, signifying a heightened potential for crack propagation under the influence of thermal-mechanical loading conditions. The increased thickness of the composite patch may also lead to a larger temperature gradient through the patch material, causing non-uniform expansion or contraction. This non-uniformity can introduce bending, distortion effects, or increased potential for delamination or other failure modes at the adhesive interface which can enhance the SIF, especially if the composite patch has a different coefficient of thermal expansion compared to the base material. These findings highlight the importance of considering patch thickness as a critical factor in the design and optimization of composite repairs, especially in environments subject to significant thermal variations.

Patch sizes

The effect of different patch sizes on the SIF under coupled thermomechanical loading demonstrates how mechanical stress, thermal expansion, and patch efficiency interact in a complex way. The findings show that, over the temperature range, the SIF values were comparatively greater for the initial 200 mm² patch size than for the 250 mm² patch size as depicted in Fig. 18. Interestingly, a discernible drop in SIF was seen when the patch size was raised to 250 mm², indicating that this size more successfully reduced the combined stresses at the crack tip. This is explained by a perfectly balanced patch stiffness and effective mechanical and thermal load distribution. In contrast, the SIF started to rise again when the patch size was extended to 300 mm² and 350 mm². At higher temperatures, the 350 mm² patch showed the greatest SIF values. When the combined effects of mechanical and thermal forces on the composite material are taken into account, this tendency can be explained. At lower temperatures, mechanical loading mostly determines the stress distribution, with temperature-induced stresses having less of an impact and similar SIF values across patch sizes. On the other hand, thermal expansion effects increase in significance with temperature. Due to differential thermal expansion between the patch and the substrate, larger patches especially those larger than the ideal size of 250 mm² may impose additional stresses, resulting in a greater SIF even with the larger patch size.

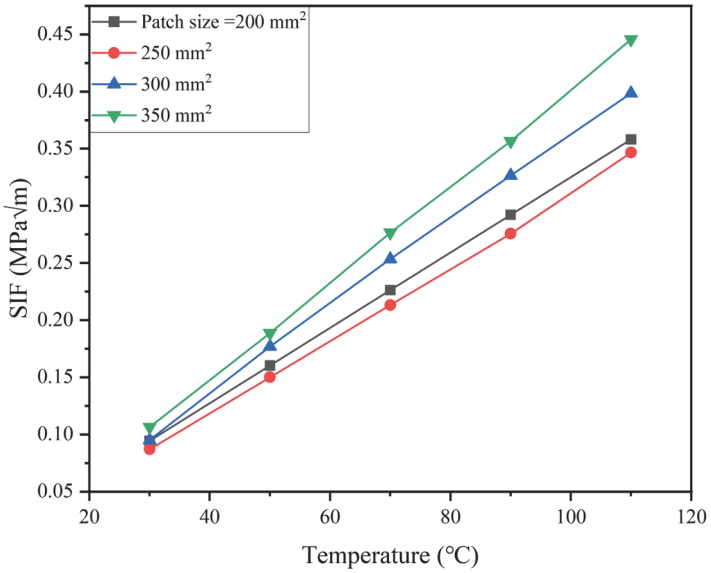

Figure 18: SIF for different patch sizes under thermo-mechanical loading.

The mismatch in thermal characteristics between the underlying structure and the patch material could perhaps be the cause of the increased SIF for larger patches at higher temperatures. Larger patches increase the area that is impacted by thermal expansion, which could result in more residual stresses in the adhesive layer and at the patch's interface with the base material. When the patch and substrate have significantly different thermal expansion coefficients, these stresses have the potential to increase stress concentration at the fracture tip. At lower temperatures, mechanical loading predominates,

but as the temperature rises, the discrepancies in SIF values become more noticeable. This is especially true for larger patch sizes, where negative thermal expansion effects outweigh the advantages of increased mechanical load distribution. The 250 mm² patch size creates a more favourable balance in stress distribution, reducing stress concentration at the crack tip more effectively than the 200 mm² size, as seen by the smaller difference in SIF between the 200 mm² and 250 mm² patches. The substantial increase in SIF values for the bigger patches (300 mm² and 350 mm²), however, indicates that thermal stresses become more prevalent, leading to increased SIF and possibly jeopardizing the efficacy of the repair.
In conclusion, the results show that SIF can be successfully decreased with a slight increase in patch size (from 200 mm² to 250 mm²) under thermo-mechanical loading. Further patch size increases, however, might cause an unfavourable rise in SIF, especially at higher temperatures. Under these circumstances, 250 mm² seems to be the ideal patch size because it offers the best balance between thermal expansion and mechanical load distribution. After this point, the mechanical benefits might be outweighed by the increasing thermal stresses, which could lead to higher SIF values and jeopardize the efficacy of the repair. This emphasizes how crucial it is to properly weigh mechanical and thermal considerations when choosing patch sizes for composite repairs in thermo-mechanical settings.

Different Patch materials

In the context of thermo-mechanical analysis, a crack of 10 mm was considered for this investigation, and the adhesive used for bonding was FM73. A comprehensive investigation was carried out to evaluate the SIF for three distinct composite materials: boron, graphite, and glass/epoxy, under varying loading conditions. The results revealed a compelling distinction in the SIF values among these materials, with the graphite composite patch demonstrating the lowest SIF, followed by boron and glass/epoxy. Intriguingly, this trend exhibited a contrasting pattern when compared to the results obtained under purely mechanical loading conditions, wherein boron/epoxy yielded the lowest SIF, followed by graphite and glass/epoxy.
The notable variation in SIF responses between mechanical and thermo-mechanical loading can be attributed to the inherent material properties of these composites, specifically their Young's modulus and coefficient of thermal expansion (CTE). In the case of mechanical loading, the structural rigidity, as denoted by young's modulus, plays a pivotal role, with boron/epoxy exhibiting the lowest SIF due to its substantial Young's modulus of 210 GPa. Conversely, under thermo-mechanical loading conditions, the CTE values become a decisive factor. Graphite's highly negative CTE of $-1.2 \times 10^{-6}/℃$ offers it an advantage, as it effectively counters the thermal expansion-induced stresses, resulting in the lowest SIF. In contrast, boron's positive CTE of $4.5 \times 10^{-6}/℃$ under these conditions contributes to higher SIF values, demonstrating the intricate interplay of material properties and loading conditions in the context of structural analysis. In contrast, glass/epoxy composites, featuring Young's modulus of 50 GPa and a CTE of $5.5 \times 10^{-6}/℃$ per degree, possess less stiffness and a higher thermal expansion rate. Consequently, their performance in both mechanical and thermo-mechanical loading conditions falls behind boron and graphite composites as its evident in Fig. 19.

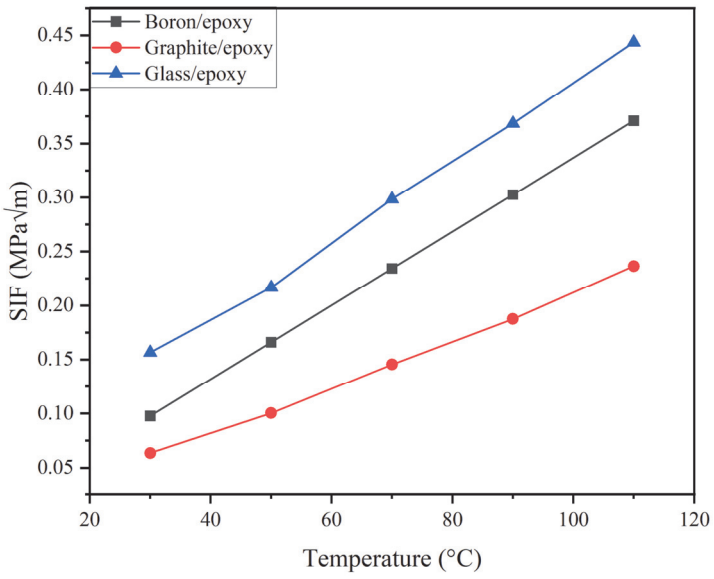

Figure 19: SIF for different patch materials under thermo-mechanical loading.

Different adhesive materials

Under thermo-mechanical loading, a similar analysis was conducted for the repair of a cracked plate with a 10 mm crack using a Boron/epoxy composite patch with three different adhesive materials: Araldite 2015, AV138, and FM73. The results, shown in Fig. 20, revealed that AV138 exhibited the lowest SIF values, followed by Araldite 2015 and FM73.

The superior performance of AV138 can be attributed to its optimal combination of mechanical properties and thermal expansion coefficient. Despite its slightly lower stiffness compared to Araldite 2015, AV138's lower coefficient of thermal expansion (CTE) results in reduced thermal stress buildup at elevated temperatures. This characteristic effectively minimizes the overall stress concentration at the crack tip, leading to lower SIF values under thermo-mechanical loading. Araldite 2015, while exhibiting a higher stiffness than AV138, has a higher CTE, which contributes to increased thermal stresses and thus higher SIF values compared to AV138. FM73, with the lowest stiffness and highest CTE among the adhesives tested, displayed the highest SIF values due to significant thermal stress concentration and reduced load-bearing capacity at elevated temperatures.

This analysis emphasizes the critical influence of adhesive properties, particularly the balance between mechanical strength and thermal expansion characteristics, on the SIF values under thermo-mechanical loading. The results highlight the importance of selecting adhesives with lower CTEs and adequate mechanical properties to enhance the structural integrity of repaired components subjected to varying thermal and mechanical loads.

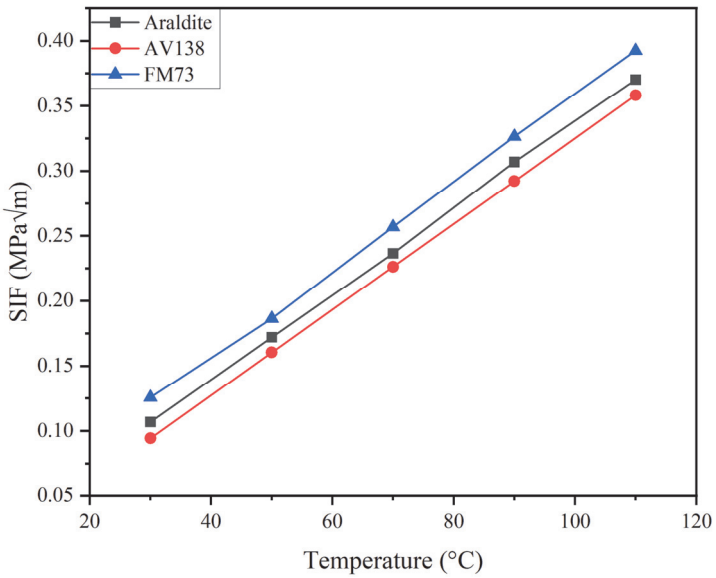

Figure 20: SIF for different adhesives under thermo-mechanical loading.

Effect of the existence of a defect in adhesive

In this segment, the plate that underwent repair with adhesive defect was exposed to thermo-mechanical loading. The analysis revealed that the influence of temperature on the efficiency of repair is more pronounced in the case of an adhesive defect compared to using regular adhesive in a thermo-mechanical environment. The elevated temperatures during thermo-mechanical loading lead to a differential expansion between the patch material, the host material, and the defected adhesive region. The adhesive defect acts as a localized defect, and with the introduction of thermal loading, the temperature-induced expansion causes the defect to expand further. This expansion exacerbates the stress concentration at the defected area, creating a larger obstacle for stress transfer from the plate to the patch.

Moreover, the thermal expansion induces additional stresses in the defected region, making it more susceptible to further propagation. This thermal expansion-driven enlargement of the defected area results in a more pronounced reduction in load-carrying capacity and a higher increase in SIF compared to the case of only mechanical loading. Therefore, under thermo-mechanical loading conditions, the combination of thermal effects and the inherent defect of adhesive defect leads to a more significant impact on the structural performance of the repaired plate compared to mechanical loading alone. Graphs depicting the impact of thermo-mechanical loading in conjunction with an adhesive defect on SIF have been generated for varying crack lengths, as illustrated in Fig. 21. At a temperature of 110°C, a crack of length, a = 10 mm produced the greatest SIF value. As indicated earlier, the defect is at the crack tip at this length of crack, and when heat is applied, the defect expands, increasing the concentration of stress at the crack tip.

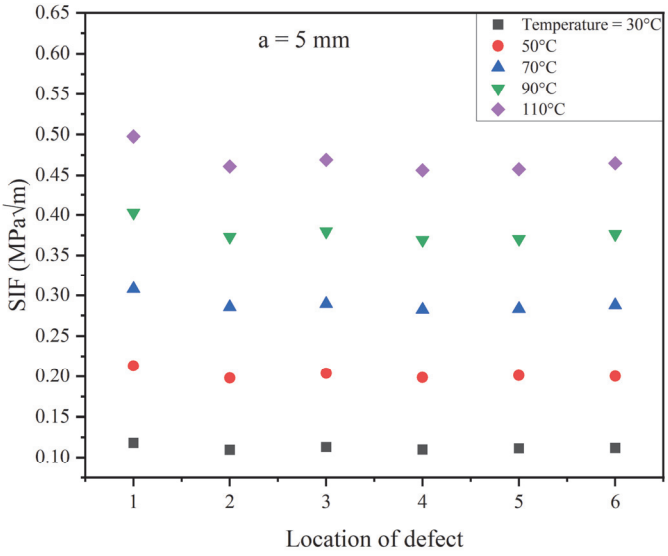

(a) 5 mm

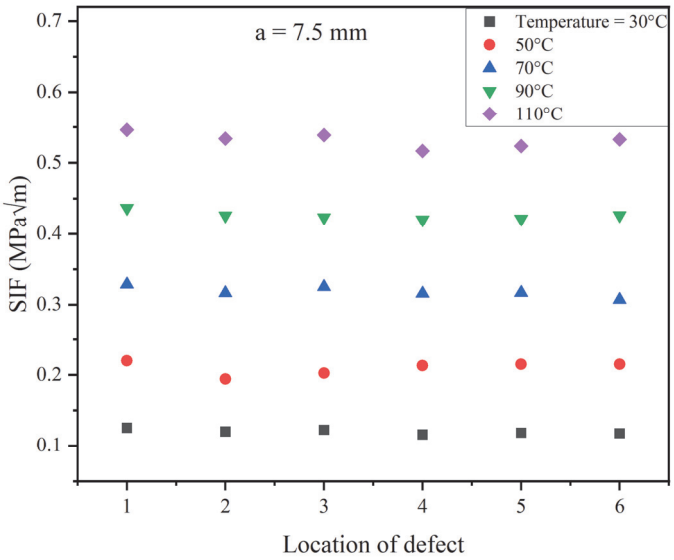

(b) 7.5 mm

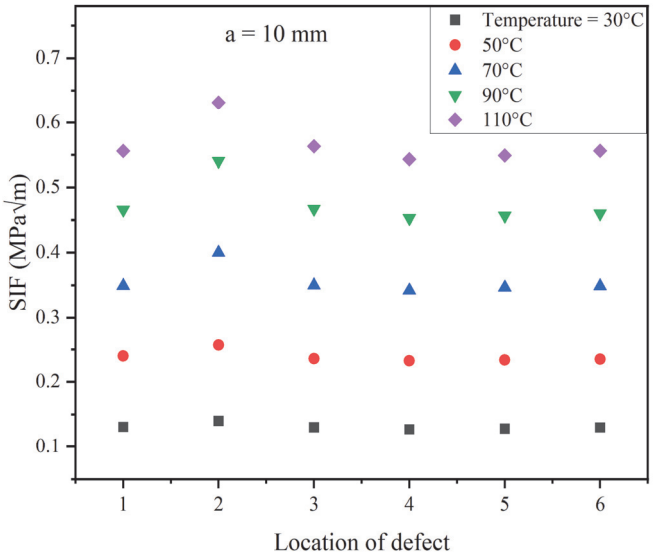

(c) 10 mm

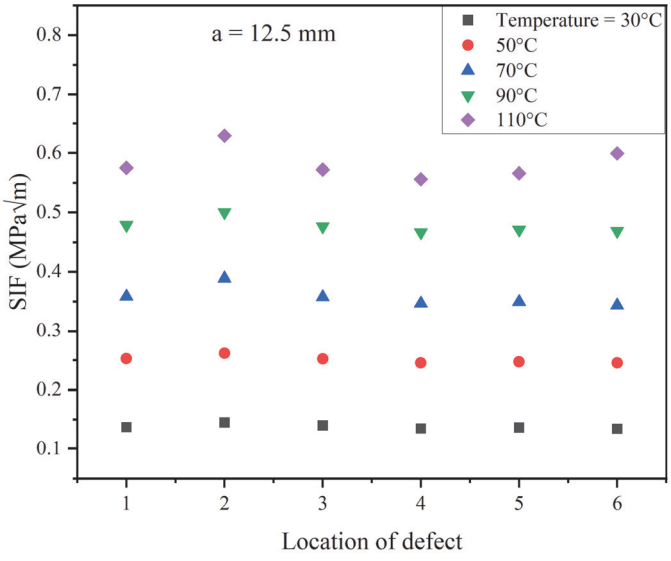

(d) 12.5 mm

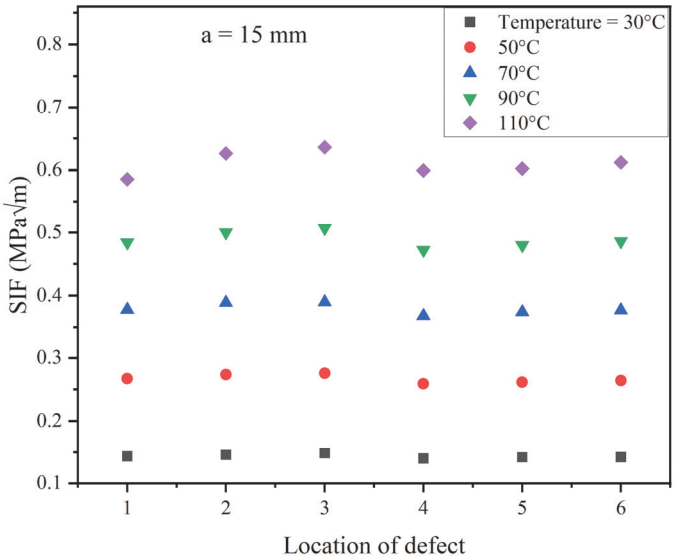

(e) 15 mm

Figure 21: Effect of adhesive defect on SIF under thermo-mech load for different crack lengths.

Deformation Analysis of Adhesive with Disbond Under Various Loading Conditions

In this section, the behaviour of the adhesive volume with a disbond under three different loading conditions: no load, mechanical load, and thermo-mechanical load is examined. The analysis highlights the deformation characteristics of the adhesive volume near the disbond region in each scenario, providing a comprehensive understanding of how various loads impact the integrity of the adhesive with an existing defect.

No Load Condition: Under no load conditions, when there is no external mechanical or thermal stress applied to the model, the adhesive volume remains in its original, undeformed state. The grid pattern in Fig. 22 representing this condition outlines the geometric configuration and boundaries of the adhesive layer near the disbonded region. In this state, the adhesive disbond is present, but there is no deformation in the adhesive volume. The absence of deformation indicates that the adhesive and the disbonded region retain their original shapes and sizes, with no induced stresses affecting the material.

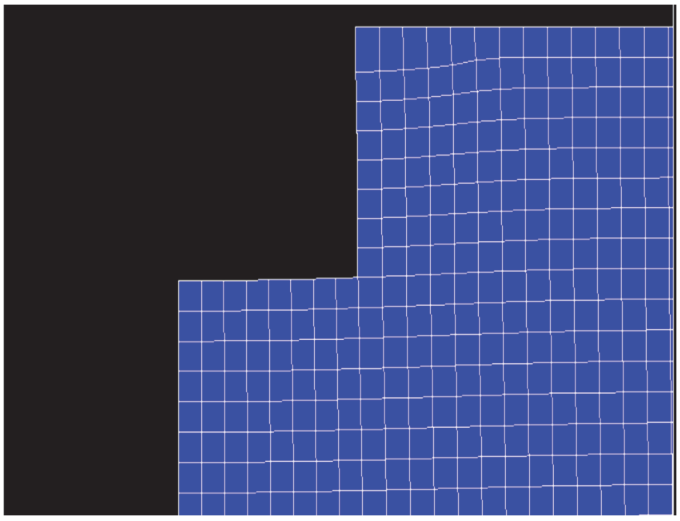

Figure 22: Adhesive volume when no load is acting on the model.

Mechanical Load Condition: When subjected to mechanical loading, the adhesive volume experiences deformation primarily in the direction of the applied mechanical load. Fig. 23 illustrates the deformation of the adhesive volume under mechanical loading. The grid pattern demonstrates a slight horizontal expansion, indicating the deformation along the y-axis, which aligns with the direction of the externally applied mechanical load. The empty grid lines transitioning to filled lines represent this deformation. This deformation, though present, is relatively small compared to thermo-mechanical loading. The mechanical load induces stress within the adhesive, causing it to deform slightly, but the deformation remains mostly aligned with the direction of the applied load.

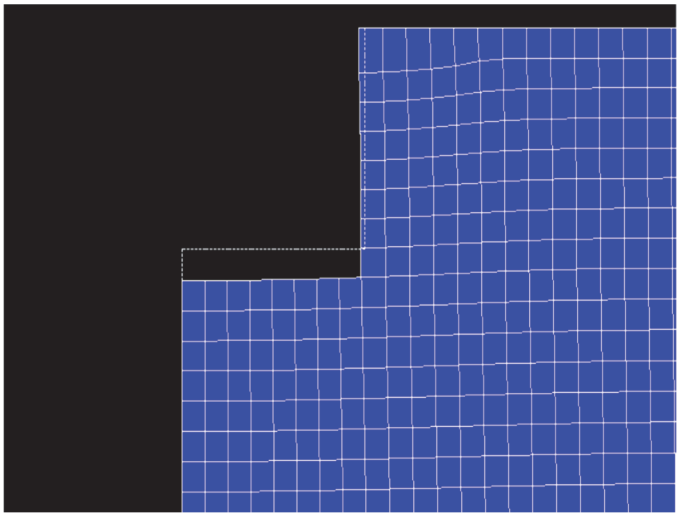

Figure 23: Deformation in adhesive volume when only mechanical load is acting on the model.

Thermo-Mechanical Load Condition: The most significant deformation is observed under thermo-mechanical loading, as shown in Fig. 24. In this condition, the adhesive volume is subjected to both high temperature and mechanical load, resulting in a complex and irregular shape change. The deformation is evident in both the x and y directions, indicating a more complex and irregular shape change. The grid lines indicate substantial displacement, highlighting the combined effects of thermal and mechanical stresses. The deformation along the y-axis is primarily due to the external mechanical load, similar to the mechanical load condition. However, the deformation along the x-axis, which is irregular in shape, is attributed to the thermal load. The thermal expansion of the adhesive material, coupled with the mechanical load, causes a more pronounced deformation. In Fig. 24, the empty spaces in the grid lines represents the amount of deformation, whereas the blue volume within the grid shows the new configuration of the adhesive disbond.

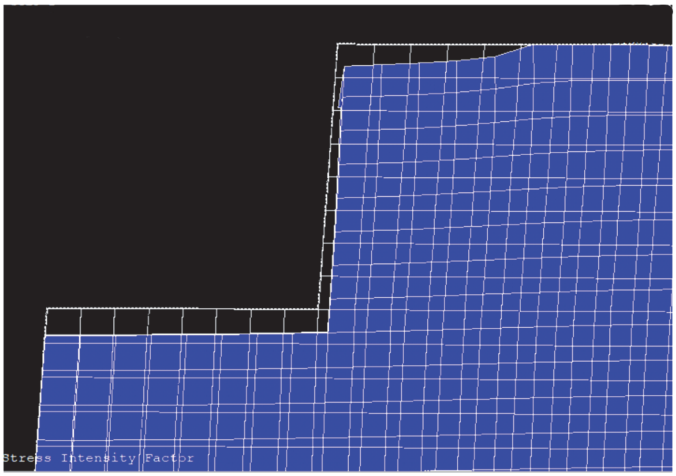

Figure 24: Deformation in adhesive volume when the thermo-mechanical load is acting on the model.

Oil Canning Effect

The deformation behaviour of the composite patch under both mechanical and thermo-mechanical loading conditions, highlights the profound impact of thermal effects, particularly regarding the oil canning phenomenon. Under pure mechanical loading, the composite patch demonstrates no deformation, maintaining a close resemblance to its original shape (represented by the dashed line) and the deformed contour as depicted in Fig. 25. This outcome suggests that the mechanical load, in isolation, does not exert enough force to induce significant deformation, thereby allowing the patch to distribute the applied stresses effectively across its surface and ensuring the stability of the repair.

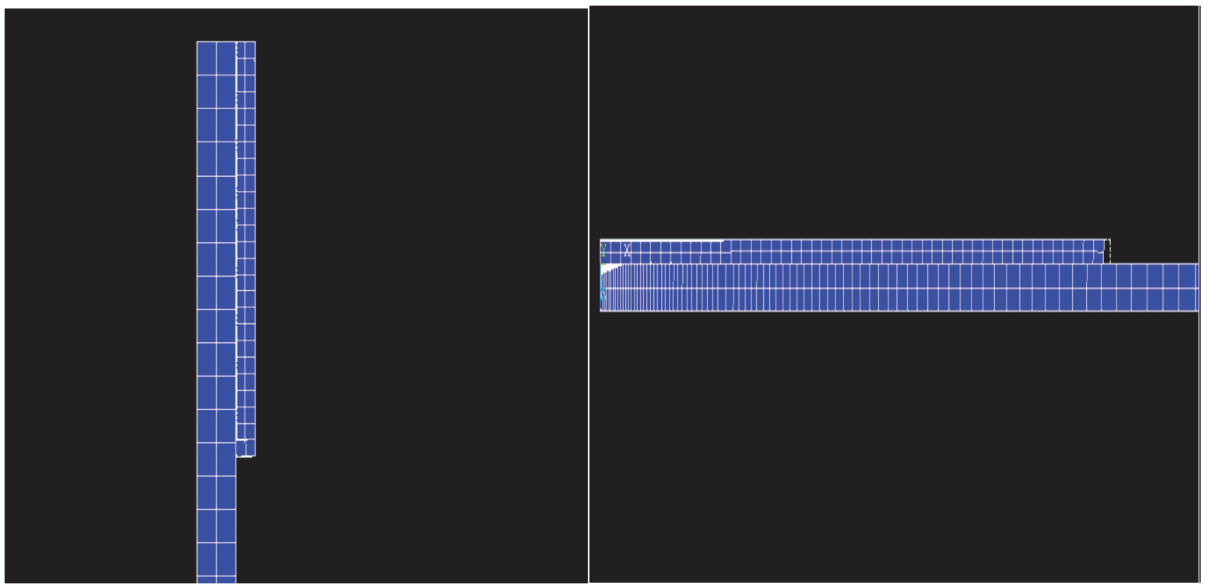

(a) (b)

Figure 25: Oil canning in the composite patch under mechanical loading (a) side view (b) top view.

In stark contrast, the introduction of thermo-mechanical loading at an elevated temperature of 110°C results in a pronounced deformation characterized by the swelling of the composite patch. This swelling is evident from the significant departure of the deformed contour from the original shape as illustrated in Fig. 26. The swelling is a clear manifestation of the oil canning effect, which arises from the differential thermal expansion between the composite patch and the underlying host plate material. Given the distinct thermal expansion coefficients of the composite material and the host structure, exposure to elevated temperatures results in uneven expansion within the patch. The patch's material properties, influenced by the high temperature, cause it to expand more than the host material, leading to localized out-of-plane deformation, or swelling, commonly referred to as oil canning.

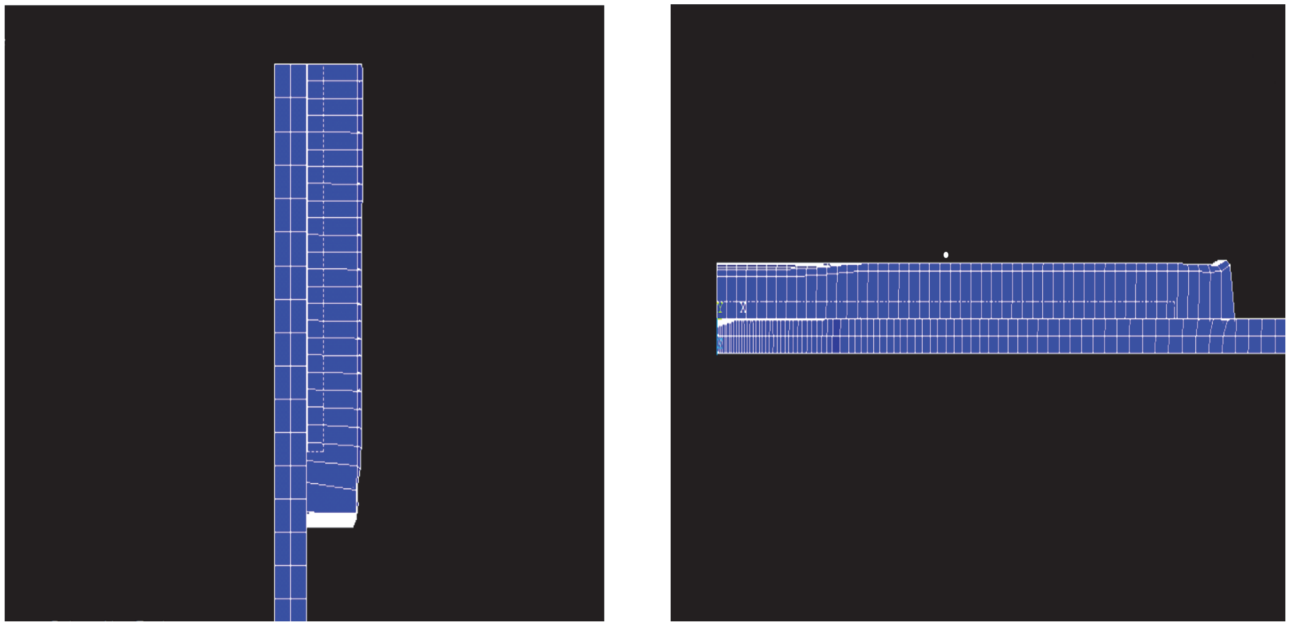

Figure 26: Oil canning in the composite patch under thermo-mechanical loading (a) side view (b) top view.

This oil canning effect under thermo-mechanical loading is significant because it alters the stress distribution across the composite patch. The localized bulging seen in the deformed shape is not just a surface anomaly but can potentially influence the overall mechanical performance of the repair. Such deformation might introduce areas of increased stress concentration, particularly around the swollen regions, which could affect the load-bearing capability of the patch. This change in stress distribution, if not properly accounted for during the design phase, might lead to compromised repair effectiveness, especially when the structure is subjected to cyclic loads over time.

Additionally, it is important to note that the oil canning effect is not a uniform deformation across the patch but rather a localized phenomenon that may vary in intensity depending on the specific geometry, material properties, and thermal history of the composite and adhesive layers. In the context of this study, the bulging observed in the composite patch under thermo-mechanical loading highlights the potential for significant deviations from expected performance if thermal effects are not adequately accounted for. The findings suggest that the interaction between thermal expansion and mechanical loading, coupled with the presence of adhesive defects, can lead to complex deformation patterns that must be understood and mitigated to ensure the long-term success of composite patch repairs in aerospace and other critical applications.

Conclusion

The study demonstrates that the efficiency of repaired plates under thermo-mechanical loading diminishes due to the generation of thermal stresses at elevated temperatures. Analysis of positive & negative temperature variations indicates a consistent increase in Stress Intensity Factor (SIF) with rising temperatures, driven by differential thermal expansion between aluminium and the composite patch. Consequently, the consideration of thermal stresses becomes paramount in the repair process. Contrary to purely mechanical loading, a consistent increase in the SIF with

rising temperatures, with increments of 18%, 36%, and 53% observed as the patch thickness increased from 0.5 mm to 1.25 mm at 110°C. This suggests that thinner patches are preferable for thermo-mechanical scenarios. While boron/epoxy patches exhibit a significant 62% reduction in SIF under purely mechanical loading, graphite/epoxy shows higher resilience under thermo-mechanical conditions, attributed to its lower coefficient of thermal expansion (CTE), which effectively mitigates thermal expansion mismatch between the patch and the parent structure. Araldite 2015 performs best under mechanical loading due to its stiffness and effective stress distribution, while AV138 exhibits superior performance under thermo-mechanical loading owing to its lower CTE and balanced mechanical properties. The presence and location of defects within the adhesive significantly impact repair performance, with defects near the crack tip posing the greatest risk. Furthermore, thermo-mechanical loading exacerbates adhesive failure at defect locations, rendering damaged adhesive unsuitable for continued service. This research casts light on the intricate interplay between material properties and varying loading conditions, offering invaluable insights to engineers and designers in their pursuit of optimizing structural performance and safety across a diverse range of operational environments. Future studies should explore more complex loading scenarios, such as cyclic loading or environmental effects, and investigate advanced materials, including hybrid composites and nanomaterials, as well as innovative repair techniques like self-healing materials. Such investigations will enhance the durability and performance of repaired aluminum structures in practical applications, contributing to safer and more efficient engineering solutions. Furthermore, optimization techniques should be employed to give recommendations for the optimal values of the different parameters to have a structure that meets the evolving requirements in the design.

ACKNOWLEDGMENT

The author Mohammed Abdulla acknowledges and thanks Kulliyyah of Engineering, International Islamic University Malaysia, for offering the KOE Postgraduate Tuition Fee Waiver Scheme. This work was supported by the Ministry of Higher Education Malaysia [grant number FRGS/1/2021/TK0/UIAM/01/5]. Also, the authors acknowledge the support of the Structures and Materials (S&M) Research Lab of Prince Sultan University.

CONFLICTS OF INTEREST

The authors declare that they have no conflicts of interest to report regarding the present study.

REFERENCES

[1] Schijve, Jaap. (2009). Fatigue of Structures and Materials. 10.1007/978-1-4020-6808-9.
[2] Fissolo, A., Amiable, S., Ancelet, O., Mermaz, F., Stelmaszyk, J.M., Constantinescu, A., Robertson, C., Vincent, L., Maillot, V. and Bouchet, F., (2009). Crack initiation under thermal fatigue: An overview of CEA experience. Part I: Thermal fatigue appears to be more damaging than uniaxial isothermal fatigue. International Journal of Fatigue, 31(3), pp.587-600.
[3] Baker, A. ed., (1988). Bonded repair of aircraft structures (7). Springer Science & Business Media.
[4] Kumar, P., (2009). Elements of fracture mechanics. McGraw-Hill Education LLC..
[5] Kassimali, A., (2005). Structural Analysis, Brooks.
[6] Davis, M. and Bond, D., (1999). Principles and practices of adhesive bonded structural joints and repairs. International journal of adhesion and adhesives, 19(2-3), pp. 91-105.
[7] Shaikh, A.A., Hriari, M. and Ali, J.S.M., (2024). Optimization of damage repair with piezoelectric actuators using the Taguchi method. Frattura ed Integrità Strutturale, 18(67), pp. 137-152.
[8] Hassan, S.F., Kundurthi, S., Vattathurvalappil, S.H., Cloud, G. and Haq, M., (2021). A hybrid experimental and numerical technique for evaluating residual strains/stresses in bonded lap joints. Composites Part B: Engineering, 225, p.109216.
[9] Mohammadi, S., Yousefi, M. and Khazaei, M., (2021). A review on composite patch repairs and the most important

parameters affecting its efficiency and durability. Journal of Reinforced Plastics and Composites, 40(1-2), pp. 3-15.
[10] Budhe, S., Banea, M.D. and de Barros, S., (2018). Bonded repair of composite structures in aerospace application: a review on environmental issues. Applied Adhesion Science, 6, pp. 1-27.
[11] Benyahia, F., Albedah, A. and Bouiadjra, B.A.B., (2014). Elliptical and circular bonded composite repair under mechanical and thermal loading in aircraft structures. Materials Research, 17, pp. 1219-1225.
[12] Schubbe, J.J., Bolstad, S.H. and Reyes, S., (2016). Fatigue crack growth behavior of aerospace and ship-grade aluminum repaired with composite patches in a corrosive environment. Composite Structures, 144, pp. 44-56.
[13] Albedah, A., Bouiadjra, B.B., Benyahia, F. and Mohammed, S.M.K., (2018). Effects of adhesive disbond and thermal residual stresses on the fatigue life of cracked 2024-T3 aluminum panels repaired with a composite patch. International Journal of Adhesion and Adhesives, 87, pp. 22-30.
[14] Kaddouri, N., Kouider, M., Amine, M.B. and Feaugas, X., (2019). Analysis of the presence of bonding defects on the fracture behavior of a damaged plate repaired by composite patch. Frattura ed Integrità Strutturale, 13(49), pp. 331-340.
[15] Mohammadi, S., (2020). Parametric investigation of one-sided composite patch efficiency for repairing crack in mixed mode considering different thicknesses of the main plate. Journal of Composite Materials, 54(22), pp. 3067-3079.
[16] Amari, K. and Berrahou, M., (2022). Experimental and numerical study of the effect of patch shape for notched cracked composite structure repaired by composite patching. Journal of Failure Analysis and Prevention, 22(3), pp. 1040-1049.
[17] Abdulla, M., Hrairi, M., Aabid, A. and Abdullah, N.A., (2024). Influence of Adhesive Curing Temperature and Geometrical Parameters on Composite Patch Repair of Cracked Structures. Journal of Advanced Research in Fluid Mechanics and Thermal Sciences, 119(1), pp. 1-12.
[18] Shaikh, A.A., Baig, M., Hrairi, M. and Ali, J.S.M., (2024). Effect of fiber orientation-based composite lamina on mitigation of stress intensity factor for a repaired plate: a finite element study: Repair of thin-walled structures. Frattura ed Integrità Strutturale, 18(68), pp. 209-221.
[19] Shaikh, A.A., Raheman, M.A., Hrairi, M. and Baig, M., (2024). Improving the performance of damage repair in thin-walled structures with analytical data and machine learning algorithms. Frattura ed Integrità Strutturale, 18(68), pp. 310-324.
[20] Abuzaid, A., Hrairi, M., Dawood, M.S.I.S. (2017). Modeling approach to evaluating reduction in stress intensity factor in center-cracked plate with piezoelectric actuator patches, J. Intell. Mater. Syst. Struct., 28(10), pp. 1334–1345, DOI: 10.1177/1045389X16672562.
[21] Grant, L.D.R., Adams, R.D. and da Silva, L.F., (2009). Experimental and numerical analysis of single-lap joints for the automotive industry. International journal of adhesion and adhesives, 29(4), pp. 405-413.
[22] Banea, M.D. and da Silva, L.F., (2009). Adhesively bonded joints in composite materials: an overview. Proceedings of the Institution of Mechanical Engineers, Part L: Journal of Materials: Design and Applications, 223(1), pp. 1-18.
[23] Anderson, T.L. and Anderson, T.L., (2005). Fracture mechanics: fundamentals and applications. CRC press.
[24] Tada, H., Paris, P.C. and Irwin, G.R., (2000). The stress analysis of cracks handbook, ed. The American Society of Mechanical Engineers.
[25] Aabid, A., Hrairi, M., Ali, J.S.M. and Abuzaid, A., (2019). Effect of bonded composite patch on the stress intensity factors for a center-cracked plate. IIUM Engineering Journal, 20(2), pp.211-221.
[26] Rose, L.R.F., (1982). A cracked plate repaired by bonded reinforcements. International Journal of Fracture, 18, pp. 135-144.
[27] Baker, A. and Aktepe, B., (2000). Sensor techniques to validate the stress intensity in cracked metallic panels repaired with bonded composite patches. Tech. rep., Defense Science and Technology Organisation, Australia.

NOMENCLATURE

SIF, K_I	stress intensity factor
CTE,α	coefficient of thermal expansion
FEM	finite element method
σ	external applied load
r	distance from crack tip
θ	angle with respect to crack plane
a	crack length

σ_0	reduced stress
Λ	characteristic crack length
σ_{xx}	normal stress in x-direction
σ_{yy}	normal stress in y-direction
τ_{xy}	shear stress
u_x	displacement in x-direction
u_y	displacement in y-direction